

MOX–Report No. 18/2007

Output functional control for nonlinear equations driven by anisotropic mesh adaption. The Navier-Stokes equations

STEFANO MICHELETTI, SIMONA PEROTTO

MOX, Dipartimento di Matematica “F. Brioschi”
Politecnico di Milano, Via Bonardi 29 - 20133 Milano (Italy)

mox@mate.polimi.it

<http://mox.polimi.it>

Output functional control for nonlinear equations
driven by anisotropic mesh adaption.
The Navier-Stokes equations*

Stefano Micheletti and Simona Perotto[‡]

29th October 2007

[‡] MOX– Modellistica e Calcolo Scientifico
Dipartimento di Matematica “F. Brioschi”
Politecnico di Milano
via Bonardi 9, 20133 Milano, Italy
{stefano.micheletti,simona.perotto}@polimi.it

Keywords: nonlinear PDE’s, output functional control, anisotropic mesh adaption, a posteriori error analysis

AMS Subject Classification: 65N15, 65N30, 65N50, 65K10

Abstract

The contribution of this paper is twofold: firstly, a general approach to the goal-oriented a posteriori analysis of nonlinear partial differential equations is laid down, generalizing the standard DWR method to Petrov-Galerkin formulations. This accounts for: different approximations of the primal and dual problems; nonhomogeneous Dirichlet boundary conditions, even different on passing from the primal to the dual problem; the error due to data approximation; the effect of stabilization (e.g. for advective-dominated problems). Secondly, moving from this framework, and employing anisotropic interpolation error estimates, a sound anisotropic mesh adaption procedure is devised for the numerical approximation of the Navier-Stokes equations by continuous piecewise linear finite elements. The resulting adaptive procedure is thoroughly addressed and validated on some relevant test cases.

*This work has been supported by COFIN 2006 “Numerical Approximation of Multiscale and Multiphysics Problems with Adaptive Methods”.

1 Introduction and motivation

In this work we set up a theoretical framework for the a posteriori error estimation to nonlinear variational problems. What we have in mind are some problems commonly met in computational science and engineering, described by partial differential equations, e.g., the Navier-Stokes equations for incompressible flows in fluid dynamics ([22]), elasto-plasticity models in solid mechanics ([24]), charge transport models in semiconductor device simulation ([31]), etc. All of these problems are actually characterized by nonlinear features. We are interested in the numerical approximation of these equations, and primarily in the estimation of the corresponding discretization error via a proper a posteriori analysis. In particular, this error is measured in terms of a suitable output functional of the solution representing derived quantities of particular engineering or scientific relevance (e.g., an averaged force on a body immersed in a fluid, a mean normal stress in a loaded material, the electric current at the terminals of a semiconductor device). Thus, in the spirit of a goal-oriented analysis, we wish to approximate, within a user-defined tolerance, the exact (but unknown) functional, evaluating the functional itself on a suitable (computable) approximation of the solution (see, e.g., [2, 5, 18, 28]). The overhead of this analysis is the introduction of an auxiliary problem, the so-called adjoint (or dual) problem. In more detail, our theoretical framework for goal-oriented a posteriori analysis provides room for: a Petrov-Galerkin approximation of the primal and dual problems that allows us to deal with nonhomogeneous Dirichlet boundary conditions, even different moving from the primal to the dual problem; the error due to the approximation of these data; the effect of stabilization, this latter being mandatory when considering finite element spaces violating the inf-sup conditions and in the presence of a high Reynolds number. A general and self-contained theory accounting for all these issues seems to be lacking in the current literature. In particular, we merge the two goal-oriented Dual Weighted Residual (DWR) approaches of [5, 18]. On the one hand, a general theory for nonlinear problems is presented in [5], however, without covering the case of Petrov-Galerkin formulations. On the other hand, [18] deals essentially with linear problems, though in the ambit of Petrov-Galerkin approximations, and the focus is drained towards postprocessing techniques of the discrete output functional for the purpose of increasing its accuracy.

After introducing the abstract setting, we firstly particularize it to the Navier-Stokes equations, and then we devise an effective technique for numerically computing a given functional associated with their solution. In this case, suitable quantities related to the fluid under investigation may be the total kinetic energy, the vorticity or the drag and lift coefficients (if the fluid flows past some immersed body). In addition, under certain conditions, for example when the Reynolds number is sufficiently high, the flow may show evident directional features, e.g., internal or boundary layers. To sharply capture these troublesome aspects without compromising the overall computational cost, an efficient rem-

edy is provided by the widely employed mesh adaption technique. With this respect, a further improvement in terms of saving on the computational cost can be achieved via an anisotropic adaptivity (see, for instance, [8, 12, 1, 11, 14, 32]). We stress that the a posteriori error estimators provide a straightforward tool for driving the mesh adaptivity.

With this aim, we combine our theoretical framework with suitable anisotropic interpolation error estimates ([14, 15]) with a view to an optimized mesh. This means that the mesh elements, each characterized by shape, orientation, and stretching, are distributed over the computational domain, such that, e.g., the number of elements is minimized for a given accuracy or, alternatively, the accuracy is maximized for a prescribed number of elements. To be practical, we may think of the above geometrical properties of the triangulation as control variables which are automatically tuned by our procedure in order to solve an optimal constrained control problem. With respect to previous works in the literature, the approach here pursued has the following advantages: it is thoroughly automatic, i.e., the user has just to enter the data for the problem and the functional at hand, and the procedure returns the approximation of the output functional along with the corresponding optimized computational mesh; the whole procedure is theoretically sound, that is, it relies on a rigorous mathematical background without resorting to any heuristic approach; the computational mesh is fully unstructured, thus providing a more flexible tool for the approximation of both the domain and the functional.

The layout of the paper comprises the start up § 2 where the main notation used throughout the paper are introduced along with the anisotropic tools employed in the later sections; the main body of the theoretical analysis is established in § 3, where the DWR approach is addressed in a Petrov-Galerkin framework, together with the corresponding a posteriori error analysis. Then we move on to considering the particular case of the Navier-Stokes equations in § 4. With a view to the numerical validation, we first illustrate the theoretical background at the basis of our adaptive procedure in § 5, and then we assess it on some test cases in § 6.

2 Preliminaries

This section is essentially meant to start up the reader on the notation used throughout the paper as well as on the anisotropic framework exploited in the a posteriori analysis of § 3.

2.1 The analytical glossary

Let us introduce the functional spaces used to guarantee the well-posedness of the problems analyzed below. For further details, we refer, for instance, to [23].

Let Ω be a polygonal domain of \mathbb{R}^2 with Lipschitz continuous boundary $\partial\Omega$. First, let $H^k(\Omega)$ denote the standard Sobolev space of functions for which the

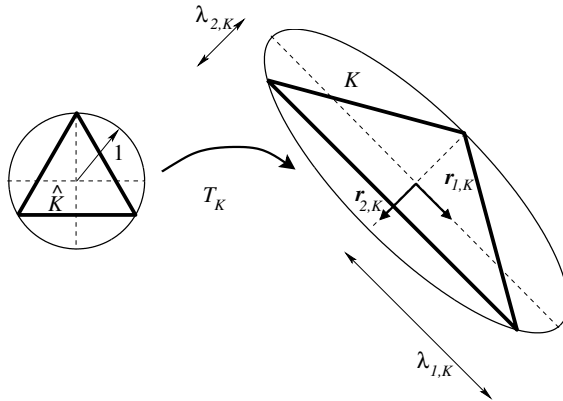


Figure 1: Geometrical interpretation of the affine map T_K and main anisotropic quantities.

distributional derivatives of order up to $k \geq 0$ is Lebesgue-square-integrable, with norm and seminorm $\|\cdot\|_{H^k(\Omega)}$ and $|\cdot|_{H^k(\Omega)}$, respectively. As first particular subset of $H^1(\Omega)$, we consider the space $H_1^1(\Omega)$ of the functions in $H^1(\Omega)$ satisfying homogeneous Dirichlet boundary conditions on a subset $\Gamma \neq \emptyset$ of $\partial\Omega$. Then the choice $k = 0$ identifies the space $L^2(\Omega)$ of the functions only Lebesgue square-integrable, with corresponding norm $\|\cdot\|_{L^2(\Omega)}$ and inner product (\cdot, \cdot) , respectively. We have to define apart the space $L^\infty(\Omega)$ of the functions bounded a.e. in Ω , as well as the space $C^0(\overline{\Omega})$ of the functions continuous on Ω . Finally the notation $\|\cdot\|_{L^2(S)}$, $\|\cdot\|_{H^k(S)}$ and $|\cdot|_{H^k(S)}$ will be adopted to refer the norms and seminorms previously defined to a proper subset S of Ω or of $\partial\Omega$.

2.2 The anisotropic *tool-box*

In this section we introduce the anisotropic setting used to enrich the a posteriori analysis below with directional information. In more detail we resort to the anisotropic framework in [14], the leading ideas being here recalled.

Let $\mathcal{T}_h = \{K\}$ be a conformal partition of Ω , consisting of triangular elements K (see, e.g., [9]). We associate with \mathcal{T}_h the finite element space of piecewise affine functions $Y_h = \{v_h \in C^0(\overline{\Omega}) : v_h|_K \in \mathbb{P}_1, \forall K \in \mathcal{T}_h\}$, with $\mathbb{P}_1 = \text{span}\{1, x_1, x_2\}$ the space of polynomials of (global) degree less than or equal to one on K . According to [14], the source of the anisotropic information is identified with the standard affine map $T_K : \widehat{K} \rightarrow K$ between the reference triangle \widehat{K} and the general one K , given by the relation

$$\vec{x} = (x_1, x_2)^T = T_K(\vec{\hat{x}}) = M_K \vec{\hat{x}} + \vec{t}_K, \quad \forall \vec{x} \in K,$$

with $\vec{\hat{x}} = (\hat{x}_1, \hat{x}_2)^T \in \widehat{K}$. For example, when \widehat{K} is picked as the equilateral triangle inscribed in the unit circle centered at the origin, with vertices

$(-\sqrt{3}/2, -1/2)$, $(\sqrt{3}/2, -1/2)$, $(0, 1)$, we may take

$$M_K = \frac{1}{3} \begin{bmatrix} \sqrt{3}(x_K^2 - x_K^1) & 2x_K^3 - x_K^1 - x_K^2 \\ \sqrt{3}(y_K^2 - y_K^1) & 2y_K^3 - y_K^1 - y_K^2 \end{bmatrix}, \quad \vec{t}_K = \frac{1}{3} \begin{bmatrix} x_K^1 + x_K^2 + x_K^3 \\ y_K^1 + y_K^2 + y_K^3 \end{bmatrix},$$

with (x_K^i, y_K^i) , for $i = 1, 2, 3$, the vertices of the triangle K .

We introduce the polar decomposition $M_K = B_K Z_K$ of M_K , where the matrix B_K is symmetric positive definite and Z_K is orthogonal (see e.g., [20]). Diagonalizing B_K in terms of its eigenvectors $\vec{r}_{i,K}$ and eigenvalues $\lambda_{i,K}$, with $i = 1, 2$, yields $B_K = R_K^T \Lambda_K R_K$, where

$$R_K = \begin{bmatrix} \vec{r}_{1,K}^T \\ \vec{r}_{2,K}^T \end{bmatrix} \quad \text{and} \quad \Lambda_K = \begin{bmatrix} \lambda_{1,K} & 0 \\ 0 & \lambda_{2,K} \end{bmatrix}.$$

The geometrical information provided by the quantities $\lambda_{i,K}, \vec{r}_{i,K}$ is displayed in Figure 1. The map T_K strains the circle circumscribed to \widehat{K} into an ellipse circumscribed to K , centered at the barycenter of K : the eigenvalues $\lambda_{1,K}, \lambda_{2,K}$ measure the length of the major and of the minor semi-axis, aligned with the directions given by $\vec{r}_{1,K}$ and $\vec{r}_{2,K}$, respectively. Notice that Z_K and \vec{t}_K do not play any role as associated with a rigid rotation and a shift, respectively.

Without loss of generality, henceforth we assume $\lambda_{1,K} \geq \lambda_{2,K}$, i.e., that the so called *stretching factor* $s_K = \lambda_{1,K}/\lambda_{2,K}$, providing us with a measure of the deformation of the triangle K , is always greater than or equal to 1, with $s_K = 1$ whenever K is an equilateral triangle.

2.2.1 Anisotropic interpolation error estimates

Moving from the above geometrical framework, we now recall some anisotropic interpolation error estimates proved in [14, 15]. They turn out to be a crucial tool with a view to the a posteriori analysis below. Moreover we point out that the adjective anisotropic understands the explicit dependence of the interpolation estimates on the geometrical parameters $\lambda_{i,K}, \vec{r}_{i,K}$ and s_K of the mesh element K in contrast with classical (isotropic) interpolation estimates, where only the diameter h_K of the element K plays a role. In particular, according to a higher or a reduced regularity of the solution at hand, we will consider the standard Lagrange interpolant as well as the Clément interpolation operator, respectively. In view of the Lagrange interpolant, for any function v such that $v|_K \in H^2(K)$, let $L_K^{i,j}(v)$ be the real number defined by

$$L_K^{i,j}(v) = \int_K (\vec{r}_{i,K}^T H_K(v) \vec{r}_{j,K})^2 dK, \quad \text{with } i, j = 1, 2, \quad (1)$$

and where $H_K(v) \in [L^2(K)]^{2 \times 2}$ is the Hessian matrix of $v|_K$ given by

$$[H_K(v)]_{i,j} = \frac{\partial^2 v}{\partial x_i \partial x_j}, \quad \text{for } i, j = 1, 2.$$

Notice that via $L_K^{i,j}(v)$ the information provided by the second-order partial derivatives, is projected along the directions $\vec{r}_{1,K}$ and $\vec{r}_{2,K}$ rather than lumped into the H^2 -seminorm $|v|_{H^2(K)}$ as in the isotropic case.

Let $\Pi_h : C^0(\bar{\Omega}) \rightarrow Y_h$ denote the Lagrange linear interpolant and let $\Pi_K : C^0(\bar{K}) \rightarrow \mathbb{P}_1$ be the corresponding restriction to K , such that $\Pi_K(v|_K) = (\Pi_h v)|_K$. Then it can be proved the following

Lemma 2.1 *Let $v \in H^1(\Omega)$ be such that $v|_K \in H^2(K)$, $\forall K \in \mathcal{T}_h$. Then there exist three constants $C_i = C_i(\hat{K})$, with $i = 1, 2, 3$, such that,*

$$\|v - \Pi_K v\|_{L^2(K)} \leq C_1 \left[\sum_{i,j=1}^2 \lambda_{i,K}^2 \lambda_{j,K}^2 L_K^{i,j}(v) \right]^{1/2}, \quad (2)$$

$$|v - \Pi_K v|_{H^1(K)} \leq C_2 \frac{1}{\lambda_{2,K}} \left[\sum_{i,j=1}^2 \lambda_{i,K}^2 \lambda_{j,K}^2 L_K^{i,j}(v) \right]^{1/2}, \quad (3)$$

$$\|v - \Pi_K v\|_{L^2(e)} \leq C_3 \left(\frac{\lambda_{1,K}^2 + \lambda_{2,K}^2}{\lambda_{2,K}^3} \right)^{1/2} \left[\sum_{i,j=1}^2 \lambda_{i,K}^2 \lambda_{j,K}^2 L_K^{i,j}(v) \right]^{1/2}, \quad (4)$$

with $e \in \partial K$ the generic edge of K .

Now let us move to the case of a less regular function, i.e. a function not necessarily continuous over $\bar{\Omega}$. For any function $v \in H^1(\Omega)$, let $G_K(v) \in \mathbb{R}^{2 \times 2}$ be the symmetric positive semi-definite matrix given by

$$[G_K(v)]_{i,j} = \int_{\Delta_K} \frac{\partial v}{\partial x_i} \frac{\partial v}{\partial x_j} dK, \quad \text{with } i, j = 1, 2,$$

and with Δ_K the union (patch) of all the elements sharing at least a vertex with K .

Let $I_h : L^2(\Omega) \rightarrow Y_h$ denote the Clément interpolant (see [10]), and let $I_K : L^2(K) \rightarrow \mathbb{P}_1$ be the corresponding restriction to K , such that $I_K(v|_K) = (I_h v)|_K$. Then the following estimates can be proved:

Lemma 2.2 *Let $v \in H^1(\Omega)$. Then under the assumptions that, for any K in \mathcal{T}_h , $\text{card}(\Delta_K) \leq M$, and $\text{diam}(\Delta_{\hat{K}}) \leq \hat{C}$, with $\Delta_{\hat{K}} = T_K^{-1}(\Delta_K)$, it holds*

$$\|v - I_K v\|_{L^2(K)} \leq C_4 \left[\sum_{i=1}^2 \lambda_{i,K}^2 (\vec{r}_{i,K}^T G_K(v) \vec{r}_{i,K}) \right]^{1/2}, \quad (5)$$

$$\|v - I_K v\|_{L^2(e)} \leq C_5 \left(\frac{h_K}{\lambda_{1,K} \lambda_{2,K}} \right)^{1/2} \left[\sum_{i=1}^2 \lambda_{i,K}^2 (\vec{r}_{i,K}^T G_K(v) \vec{r}_{i,K}) \right]^{1/2}, \quad (6)$$

where $C_i = C_i(M, \hat{C})$, for $i = 4, 5$.

Notice the explicit dependence of all the estimates above on the anisotropic quantities highlighted in Figure 1. In particular, when $\lambda_{1,K} \simeq \lambda_{2,K} \simeq h_K$, that is when the triangle is equilateral, (2)-(4), (5)-(6) reduce to the corresponding standard isotropic results (see, for instance, [9]).

Remark 2.1 *The reference patch $\Delta_{\hat{K}}$ is obtained by mapping back all the elements $T \in \Delta_K$ by means of the same transformation T_K^{-1} . The conditions constraining estimates (5) and (6) essentially avoid too distorted patches in the reference framework. On the other hand, they do not limit the anisotropic features (stretching factor and orientation) of each $T \in \Delta_K$, but rather the variation over Δ_K of the geometrical quantities of Figure 1 (see [27] for more details). Finally the constants C_4 and C_5 in (5) and (6) are an $\mathcal{O}(M, \hat{C})$ as, according to the analysis in [14], all the interpolation estimates above are actually derived in the reference setting and then mapped back to the general one.*

3 Goal-oriented a posteriori analysis

In this section we establish the theoretical framework of the pursued goal-oriented analysis on grounds of the standard dual-based a posteriori setting. In particular our approach turns out quite general as including nonlinear problems, generalized Galerkin approximation (e.g., stabilized formulations), different functional spaces for the primal and dual problems (in the spirit of a Petrov-Galerkin method), as well as nonhomogeneous Dirichlet data. For this purpose, we combine the Dual Weighted Residual (DWR) approach of [5] with the theory in [18]. The later analysis of the Navier-Stokes equations will exactly fit this abstract environment.

In more detail, after providing some concepts and notation handy for the a posteriori analysis, we introduce the DWR approach from which we move in view of the desired error estimator.

3.1 Some notation

In the sequel we deal essentially with semilinear forms defined on some linear space V . More precisely, with the notation $b(u)(\cdot, \dots, \cdot) : V \times V \times \dots \times V \rightarrow \mathbb{R}$ it is understood that the form $b(u)(\cdot, \dots, \cdot)$ is nonlinear with respect to the argument in the first bracket while it depends linearly on all the arguments in the second one.

Let us recall the definition of the Gâteaux derivative of a given form $b(u)(\cdot, \dots, \cdot)$, depending linearly, for instance, on i arguments. We have to distinguish between the derivative with respect to the first argument and the derivatives with respect to the arguments in the second bracket. In the first case, we get a linear operator $b'(u)(\cdot, \dots, \cdot, \cdot) : V \times V \times \dots \times V \times V \rightarrow \mathbb{R}$ linearly dependent on $(i+1)$ -arguments,

which, evaluated on φ is provided by the relation

$$b'(u)(\cdot, \dots, v, \underbrace{\varphi}_{(i+1)\text{-th}}) = \lim_{\varepsilon \rightarrow 0} \frac{1}{\varepsilon} \left[b(u + \varepsilon\varphi)(\cdot, \dots, \underbrace{v}_{i\text{-th}}) - b(u)(\cdot, \dots, \underbrace{v}_{i\text{-th}}) \right]. \quad (7)$$

On the other hand, the derivative of $b(u)(\cdot, \dots, \cdot)$ with respect to the j -th linear argument, say v , with $1 \leq j \leq i$, is given by

$$b(u)(\cdot, \dots, \underbrace{\phi}_{j\text{-th}}, \dots, \cdot) = \lim_{\varepsilon \rightarrow 0} \frac{1}{\varepsilon} \left[b(u)(\cdot, \dots, \underbrace{v + \varepsilon\phi}_{j\text{-th}}, \dots, \cdot) - b(u)(\cdot, \dots, \underbrace{v}_{j\text{-th}}, \dots, \cdot) \right] \quad (8)$$

when evaluated on φ . Notice that, in the case of (8) the resulting derivative returns the operator b itself while the number of arguments in the second bracket remains equal to i . On the contrary in the case of (7), this number increases to $i + 1$, thus being $b' \neq b$.

Further, suppose that V and W are two real Hilbert spaces with norms $\|\cdot\|_V$ and $\|\cdot\|_W$, respectively and that $V_0 \subseteq V$ and $W_0 \subseteq W$ are two corresponding real Hilbert subspaces, still equipped with the norms $\|\cdot\|_V$ and $\|\cdot\|_W$. Now if V_0 is a proper subspace of V and c is a fixed element of V , we define the affine space $V_c = c + V_0$ of the elements which can be written as $c + v$, with $v \in V$; similarly, if W_0 is a proper subspace of W and $d \in W$ is fixed, we let $W_d = d + W_0$. Of course, if $c \in V_0$ then, by linearity, $V_c = V_0$; likewise, if $d \in W_0$ then $W_d = W_0$. Finally, we denote by V' the dual of a Hilbert space V , and the duality pairing between V' and V is designated by ${}_V \langle \cdot, \cdot \rangle_V$.

3.2 The DWR approach

Let $J(u)$ be the goal quantity we are interested in and let $J(u_h)$ be a corresponding computable approximation, with $J(\cdot)$ a continuous functional, possibly nonlinear, u and u_h the exact and the approximate solution to the problem at hand, respectively. Several instances of the functional $J(\cdot)$ have been proposed during the last twenty years in the literature. In the CFD framework typical examples are the kinetic energy or the vorticity of a fluid, the lift or drag in a flow past a body; in structural mechanics $J(\cdot)$ can represent the torsion moment, rather than the stress values or the total surface tension, and so on.

We now introduce the abstract setting from which the goal-oriented analysis in §3.3 stems. The basic idea to estimating the functional error $J(u) - J(u_h)$ relies on embedding the given problem into the framework of optimal control. The notation adopted in the sequel are compliant with §3.1.

Let us assume that the problem at hand, henceforth denoted by *primal problem*, is represented by the strong form

$$\mathcal{A}(u) = f \quad \text{in } W', \quad (9)$$

for the unknown $u \in V$, with $\mathcal{A} : V \rightarrow W'$ a given nonlinear operator, $f \in W'$ the source term, supplied with suitable boundary conditions, compatible with $\mathcal{A}(\cdot)$. With (9) it is associated the weak form: find $u \in V_c \subseteq V$ such that

$$a(u)(\varphi) = F(\varphi) \quad \forall \varphi \in W_0 \subseteq W, \quad (10)$$

where $a(\cdot)(\cdot) : V \times W \rightarrow \mathbb{R}$, $F(\cdot) : W \rightarrow \mathbb{R}$ are suitable semilinear and linear forms, respectively. Typically it holds that $V \equiv W \equiv [H^1(\Omega)]^n$, for some integer $n \geq 1$, while the subspaces V_c and W_0 hinge on the boundary conditions assigned to the problem at hand. In practice, the existence and the uniqueness of the solution u in V_c to the variational equation (10) has to be guaranteed: the argument used for this purpose is outside the present framework. Here, we only assume that the form $a(\cdot)(\cdot)$ is sufficiently regular on $V_c \times W_0$ so that the solution u is uniquely determined and depends continuously on the data of the problem.

Let $J(\cdot) : V \rightarrow \mathbb{R}$ be the (linear or nonlinear) functional identifying the goal quantity we are interested in.

The key point is that the solution of (10) can be equivalently characterized as the solution of the following (trivial) *constrained optimization problem*: find $u \in V_c \subseteq V$ such that

$$J(u) = \min_{v \in M} J(v) \quad (11)$$

with $M = \{v \in V_c : a(v)(w) = F(w), \forall w \in W_0\}$. The problem is trivial as the space of the constraints M consists of only one element, that is $M = \{u\}$, so that (11) is equivalent to evaluating $J(u)$ on the solution to the primal problem. Let us solve the minimization problem (11) via the Lagrangian approach. With this aim we momentarily neglect the boundary conditions and we introduce the Lagrangian $\mathcal{L} : V \times W \rightarrow \mathbb{R}$, such that

$$\mathcal{L}(u, z) = J(u) + F(z) - a(u)(z) \quad \forall (u, z) \in V \times W, \quad (12)$$

with z the so-called Lagrangian multiplier (or influence function). As the minimum u coincides with the first component of the saddle point (u, z) of the Lagrangian \mathcal{L} , we are interested in finding the critical points of \mathcal{L} , that is the pair $(u, z) \in V \times W$ satisfying the Euler-Lagrange relation

$$\mathcal{L}'(u, z)(\psi, \varphi) = J'(u)(\psi) + F(\varphi) - a(u)(\varphi) - a'(u)(z, \psi) = 0, \quad \forall (\psi, \varphi) \in V \times W, \quad (13)$$

$\mathcal{L}'(u, z)(\psi, \varphi)$ denoting the derivative of the Lagrangian $\mathcal{L}(u, z)$ applied to (ψ, φ) . Coming back to the specific problem (10), we have to rewrite relation (13) on suitable subspaces taking into account the boundary conditions on the primal problem as well as the possibly different dual boundary conditions: find $(u, z) \in V_c \times W_d$ such that

$$\mathcal{L}'(u, z)(\psi, \varphi) = J'(u)(\psi) + F(\varphi) - a(u)(\varphi) - a'(u)(z, \psi) = 0, \quad \forall (\psi, \varphi) \in V_0 \times W_0, \quad (14)$$

with $W_d \subseteq W$. Relation (14) returns the primal problem (10) and the so-called *adjoint problem* to be solved for the Lagrangian multiplier: find $z \in W_d \subseteq W$ such that

$$a'(u)(z, \psi) = J'(u)(\psi) \quad \forall \psi \in V_0 \subseteq V. \quad (15)$$

As for the primal problem, the existence of the adjoint solution z satisfying (15) is separately proved via proper arguments depending on the problem at hand. The strong form of the dual problem is given by

$$\mathcal{A}'(u)^* z = j \quad \text{in } V', \quad (16)$$

reinforced with appropriate (adjoint) boundary conditions, where

$$\mathcal{A}'(u)v = \lim_{\varepsilon \rightarrow 0} \frac{1}{\varepsilon} \left[\mathcal{A}(u + \varepsilon v) - \mathcal{A}(u) \right] \quad \forall v \in V,$$

is the Jacobian of \mathcal{A} , evaluated at u and acting on v , while $\mathcal{A}'(u)^*$ is the linear operator obtained by computing the formal adjoint of $\mathcal{A}'(u)$ via the Lagrange identity ([25])

$${}_W \langle \mathcal{A}'(u)v, w \rangle_W = {}_{V'} \langle v, \mathcal{A}'(u)^* w \rangle_{V'} \quad \forall (v, w) \in V \times W. \quad (17)$$

The quantity $j \in V'$ in (16) represents the density function associated with $J'(u)(\cdot)$ such that

$$J'(u)(\psi) = {}_{V'} \langle j, \psi \rangle_{V'}, \quad \forall \psi \in V.$$

Let us now deal with the discrete counterpart. Suppose that $\{V_{0,h}\}_h$ and $\{W_{0,h}\}_h$ are two families of finite-dimensional subspaces of V_0 and W_0 , respectively, parameterized by $h \in (0, 1]$. When V_0 is a proper Hilbert subspace of V , we consider the affine variety $V_{c,h} = c_h + V_{0,h} \not\subseteq V_c$, where c_h is a suitable approximation of c , obtained, e.g., by interpolation or projection. In the same fashion, when W_0 is a proper subspace of W , we introduce the affine variety $W_{d,h} = d_h + W_{0,h} \not\subseteq W_d$, d_h being an approximation to d . Essentially we are dealing with a non-conforming approximate formulation. In the present setting, the discrete formulations and the corresponding error analysis are nontrivial due to both *data approximation*, i.e. the approximation of c, d by c_h, d_h , respectively, and to *stabilization*. This latter is mandatory when considering finite element spaces violating the inf-sup conditions and in the presence of a large Reynolds number.

The discrete counterpart of the Euler-Lagrange equations (14) reads: find $(u_h, z_h) \in V_{c,h} \times W_{d,h}$ such that

$$\mathcal{L}'(u_h, z_h)(\psi_h, \varphi_h) + \langle \mathcal{R}(u_h, z_h), \mathcal{S}(u_h)(\psi_h, \varphi_h) \rangle_\tau = 0 \quad \forall (\psi_h, \varphi_h) \in V_{0,h} \times W_{0,h}, \quad (18)$$

where the stabilization term $\langle \cdot, \cdot \rangle_\tau$ is to be understood as

$$\langle \cdot, \cdot \rangle_\tau = \sum_{K \in \mathcal{T}_h} \tau_K(\cdot, \cdot)_{L^2(K)}, \quad (19)$$

for convenient piecewise constant stabilization parameters τ_K (see, e.g., [4]). With

$$\mathcal{R}(u, z) = \begin{bmatrix} f - \mathcal{A}(u) \\ j - \mathcal{A}'(u)^* z \end{bmatrix}$$

we denote the strong form of both the primal and dual residuals, while

$$\mathcal{S}(u_h)(\psi_h, \varphi_h) = \begin{bmatrix} \mathcal{S}_p(u_h) \varphi_h \\ \mathcal{S}_d(u_h) \psi_h \end{bmatrix} \quad \forall (\psi_h, \varphi_h) \in V_{0,h} \times W_{0,h}, \quad (20)$$

collects appropriate stabilizing operators for both the primal (\mathcal{S}_p) and the dual (\mathcal{S}_d) problems, evaluated at u_h . For example, in the case of Galerkin Least Squares (GALS) stabilization ([16]), it holds $\mathcal{S}_p(u_h) = \mathcal{A}(u_h)$ while $\mathcal{S}_d(u_h) = \mathcal{A}'(u_h)^*$. Another choice corresponding to the so-called *subgrid stabilization*, mentioned in [4] and derived in the Appendix, may be adopted. Thus, via (18), the actual primal and dual discrete problems read: find $(u_h, z_h) \in V_{c,h} \times W_{d,h}$ such that

$$\begin{aligned} F(\varphi_h) - a(u_h)(\varphi_h) + \langle f - \mathcal{A}(u_h), \mathcal{S}_p(u_h) \varphi_h \rangle_\tau &= 0 \quad \forall \varphi_h \in W_{0,h}, \\ J'(u_h)(\psi_h) - a'(u_h)(z_h, \psi_h) + \langle j - \mathcal{A}'(u_h)^* z_h, \mathcal{S}_d(u_h) \psi_h \rangle_\tau &= 0 \quad \forall \psi_h \in V_{0,h}. \end{aligned} \quad (21)$$

We are now in a position to address the a posteriori error analysis.

3.3 The a posteriori analysis

In view of estimating the discretization error $J(u) - J(u_h)$ on the functional of interest $J(\cdot)$, we move from a corresponding *exact* representation, generalizing the theory in [5].

Proposition 3.1 *Let u and u_h be the solution to the weak and to the discrete primal problem (10) and (21)₁, respectively, and z_h be the solution to the discrete dual problem (21)₂. Then it holds*

$$\begin{aligned} J(u) - J(u_h) &= \underbrace{\mathcal{L}(u, z) - \mathcal{L}(u_h, z_h)}_A + \underbrace{a(u)(d) - a(u_h)(d_h) - F(d - d_h)}_B \\ &\quad - \underbrace{\langle f - \mathcal{A}(u_h), \mathcal{S}_p(u_h)(z_h - d_h) \rangle_\tau}_C. \end{aligned} \quad (22)$$

Proof. From (12), evaluating $\mathcal{L}(\cdot, \cdot)$ first at (u, z) and then at (u_h, z_h) , and properly rearranging the terms, we have

$$J(u) - J(u_h) = \mathcal{L}(u, z) + a(u)(z) - F(z) - \mathcal{L}(u_h, z_h) - a(u_h)(z_h) + F(z_h). \quad (23)$$

From (10), choosing $\varphi = z - d \in W_0$, we obtain

$$a(u)(z) - F(z) = a(u)(d) - F(d), \quad (24)$$

while, using the discrete primal problem (21)₁ with $\varphi_h = z_h - d_h \in W_{0,h}$ yields

$$F(z_h) - a(u_h)(z_h) = F(d_h) - a(u_h)(d_h) - \langle f - \mathcal{A}(u_h), \mathcal{S}_p(u_h)(z_h - d_h) \rangle_\tau. \quad (25)$$

Substituting (24) and (25) into (23) allows us to rewrite the error on the goal functional $J(\cdot)$ as in (22). \square

Notice the different meaning of the terms in the right-hand side of (22): the first one A is associated with the Galerkin approximation procedure only, so that we may name it *Galerkin defect*; the quantity B is due to data approximation and it vanishes when $d = d_h$ and $d_h \in W_{0,h}$, while the last term C is related to stabilization.

We now provide an alternative expression for the Galerkin defect term.

Proposition 3.2 *Let $e_u = u - u_h$ and $e_z = z - z_h$ be the primal and the dual discretization error, respectively. Then the Galerkin defect term can be rewritten as*

$$\begin{aligned} \mathcal{L}(u, z) - \mathcal{L}(u_h, z_h) &= \frac{1}{2} \left[\mathcal{L}'(u_h, z_h)(e_u, e_z) + \underbrace{F(d - d_h) - a(u)(d - d_h)}_D \right. \\ &\quad \left. + \underbrace{J'(u)(c - c_h) - a'(u)(z, c - c_h)}_E \right] + R^{(3)}, \end{aligned} \quad (26)$$

where the remainder

$$R^{(3)} = \frac{1}{2} \int_0^1 \mathcal{L}'''(u_h + se_u, z_h + se_z)(e_u, e_z, e_u, e_z, e_u, e_z) s(1-s) ds \quad (27)$$

is a third order term with respect to both e_u and e_z .

Proof. Using simple calculus, we have

$$\begin{aligned} \mathcal{L}(u, z) - \mathcal{L}(u_h, z_h) &= \int_0^1 \mathcal{L}'(u_h + s(u - u_h), z_h + s(z - z_h))(e_u, e_z) ds \\ &\quad - \frac{1}{2} [\mathcal{L}'(u_h, z_h)(e_u, e_z) + \mathcal{L}'(u, z)(e_u, e_z)] + \frac{1}{2} \mathcal{L}'(u_h, z_h)(e_u, e_z) \\ &\quad + \frac{1}{2} \mathcal{L}'(u, z)(c - c_h + e_{0,u}, d - d_h + e_{0,z}), \end{aligned} \quad (28)$$

where we have split the errors as $e_u = c - c_h + e_{0,u}$, $e_z = d - d_h + e_{0,z}$, with $e_{0,u} \in V_0$ and $e_{0,z} \in W_0$. Moreover, using the Euler-Lagrange equations (14), it holds

$$\mathcal{L}'(u, z)(c - c_h + e_{0,u}, d - d_h + e_{0,z}) = J'(u)(c - c_h) + F(d - d_h) - a(u)(d - d_h) - a'(u)(z, c - c_h).$$

Result (26) follows on recognizing in the second term at the right-hand side of (28) the approximation of the integral coinciding with the first term via the trapezoidal quadrature rule, the corresponding remainder being given by (27). \square

We remark that the terms D and E at the right-hand side of (26) may be thought of as residual-like quantities associated with the primal and the dual

problem, respectively, taking into account the non-conformity of the adopted discretization framework. In particular, they vanish only when $c - c_h \in V_0$ and $d - d_h \in W_0$, i.e. when the spaces $V_{c,h}$ and $W_{d,h}$ are subset of V_c and W_d , respectively.

In view of a compact notation, let us introduce the so-called primal $\rho_p : W \rightarrow \mathbb{R}$ and dual $\rho_d : V \rightarrow \mathbb{R}$ *weak residuals*, given by

$$\rho_p(\cdot) = F(\cdot) - a(u_h)(\cdot), \quad \rho_d(\cdot) = J'(u_h)(\cdot) - a'(u_h)(z_h, \cdot), \quad (29)$$

measuring the failure of the discrete solutions u_h and z_h at satisfying the weak primal and dual problem, respectively. The two residuals $\rho_p(\cdot)$ and $\rho_d(\cdot)$ are generally equal in the presence of a thoroughly linear problem, when a standard Galerkin approximation is adopted and the same choice is done for the primal and dual spaces. On the contrary this is not yet guaranteed when the problem at hand is nonlinear. In both the cases it is always possible to relate one another the two residuals (see [5]). Nevertheless, if one exploits this relation in view of a final estimate written in terms of only one out of the two residuals, the remainder term $R^{(3)}$ turns out to be only second order in the discretization errors instead of third order.

We can thus state the final result of this abstract goal-oriented setting, represented by the following

Proposition 3.3 *Let u and u_h be the solution to the weak and to the discrete primal problem (10) and (21)₁, respectively, and z_h be the solution to the discrete dual problem (21)₂. Then the following identity holds:*

$$\begin{aligned} J(u) - J(u_h) &= \underbrace{\frac{1}{2}\rho_p((\mathcal{I} - \mathcal{P}_W)e_{0,z}) + \frac{1}{2}\rho_d((\mathcal{I} - \mathcal{P}_V)e_{0,u})}_{\text{I}} + \underbrace{\frac{1}{2}\rho_p(d - d_h)}_{\text{II}} \\ &+ \underbrace{\frac{1}{2}\rho_d(c - c_h)}_{\text{III}} - \underbrace{\frac{1}{2}\langle \mathcal{R}(u_h, z_h), \mathcal{S}(u_h)(\mathcal{P}_V e_{0,u}, \mathcal{P}_W e_{0,z}) \rangle_\tau}_{\text{IV}} + \underbrace{[a(u)(d_h) - a(u_h)(d_h)]}_{\text{V}} \\ &+ \underbrace{\frac{1}{2}[a(u)(d - d_h) - F(d - d_h)]}_{\text{VI}} - \underbrace{\langle f - \mathcal{A}(u_h), \mathcal{S}_p(u_h)(z_h - d_h) \rangle_\tau}_{\text{VII}} \\ &+ \underbrace{\frac{1}{2}[J'(u)(c - c_h) - a'(u)(z, c - c_h)]}_{\text{VIII}} + \underbrace{R^{(3)}}_{\text{IX}}, \end{aligned} \quad (30)$$

with $\rho_p(\cdot)$ and $\rho_d(\cdot)$ the residuals defined in (29), \mathcal{I} the identity operator, $R^{(3)}$ the remainder term in (27), $e_{0,u}, e_{0,z}$ the “homogeneous” components of the primal (e_u) and of the dual (e_z) discretization error, respectively, and where \mathcal{P}_V and \mathcal{P}_W denote suitable interpolation operators.

Proof. First we combine Propositions 3.1 and 3.2, summing (18) after multiplication by one half. This yields the identity

$$\begin{aligned}
J(u) - J(u_h) &= \frac{1}{2} \mathcal{L}'(u_h, z_h)(e_u + \psi_h, e_z + \varphi_h) + \frac{1}{2} \langle \mathcal{R}(u_h, z_h), \mathcal{S}(u_h)(\psi_h, \varphi_h) \rangle_\tau \\
&\quad + a(u)(d) - a(u_h)(d_h) - F(d - d_h) + \frac{1}{2} [F(d - d_h) - a(u)(d - d_h)] \\
&\quad + \frac{1}{2} [J'(u)(c - c_h) - a'(u)(z, c - c_h)] - \langle f - \mathcal{A}(u_h), \mathcal{S}_p(u_h)(z_h - d_h) \rangle_\tau + R^{(3)},
\end{aligned} \tag{31}$$

$\forall (\psi_h, \varphi_h) \in V_{0,h} \times W_{0,h}$. Now, the second line in (31) can be rewritten as

$$\frac{1}{2} [a(u)(d - d_h) - F(d - d_h)] + [a(u)(d_h) - a(u_h)(d_h)],$$

namely as a term due to data approximation, vanishing when $d - d_h \in W_0$, summed to a second one linked, somehow, to the well-known Galerkin orthogonality property and identically equal to zero for $d_h \in W_{0,h}$ in the absence of stabilization.

We now choose in (31) the arbitrary test functions (ψ_h, φ_h) by picking $\psi_h = -\mathcal{P}_V e_{0,u} \in V_{0,h}$ and $\varphi_h = -\mathcal{P}_W e_{0,z} \in W_{0,h}$, with \mathcal{P}_V and \mathcal{P}_W interpolant operators properly chosen according to the problem at hand.

Then result (30) immediately follows after recalling the explicit expression (14) of the Lagrange derivative, the error decompositions $e_u = c - c_h + e_{0,u}$, $e_z = d - d_h + e_{0,z}$, with $e_{0,u} \in V_0$, $e_{0,z} \in W_0$, and exploiting the definition (29) of the weak residuals. \square

We underline that we are still dealing with the exact expression of the goal error $J(u) - J(u_h)$, no upper bound being involved at this stage. Moreover, with a view to the a posteriori analysis of § 4.1, we anticipate that just the first term I in (30), being the only one significant for an anisotropic grid adaption, will be employed to drive the adaptive procedure.

Remark 3.1 *The stabilization term $\langle f - \mathcal{A}(u_h), \mathcal{S}_p(u_h)(z_h - d_h) \rangle_\tau$ at the right-hand side of (31) is thoroughly computable as depending only on the discrete solutions u_h and z_h and on some known data. One can consequently identify this term with a correction quantity, say \tilde{J} , so that the new corrected functional $J_{\text{corr}} = J(u_h) - \tilde{J}$ can be exploited to estimate the goal-quantity $J(u)$, sharing the same spirit as the functional correction approach reviewed in [18]. However this approach will not be pursued in the following.*

We are now ready for introducing the Navier-Stokes equations and the associated goal-oriented a posteriori analysis, perfectly fitting the general framework just settled.

4 The Navier-Stokes equations

Let us consider the standard Navier-Stokes equations for an incompressible fluid completed with mixed boundary conditions:

$$\begin{cases} -\nabla \cdot \boldsymbol{\sigma} + (\vec{v} \cdot \nabla) \vec{v} = \vec{f} & \text{in } \Omega, \\ \nabla \cdot \vec{v} = 0 & \text{in } \Omega, \\ \boldsymbol{\sigma} \vec{n} = \vec{g} & \text{on } \Gamma_N, \\ \vec{v} = \vec{v}_D & \text{on } \Gamma_D, \end{cases} \quad (32)$$

where the stress rate $\boldsymbol{\sigma} = \boldsymbol{\sigma}(\vec{v}, p) = 2\mu \boldsymbol{\epsilon}(\vec{v}) - p\mathbf{I}$ depends on the velocity \vec{v} and on the pressure p , while $\mu > 0$ is the kinematic viscosity, $\boldsymbol{\epsilon}(\vec{v}) = \frac{1}{2}(\nabla \vec{v} + (\nabla \vec{v})^T)$ represents the strain rate, and \mathbf{I} denotes the identity tensor. The 1D-varieties Γ_D and Γ_N , with $\Gamma_D \neq \emptyset$, coincide with two disjoint boundary portions such that $\overline{\Gamma_D} \cup \overline{\Gamma_N} = \partial\Omega$ and $\Gamma_D \cap \Gamma_N = \emptyset$. Notice that Γ_D as well as Γ_N may each comprise disjoint subsets of the boundary. Concerning the data problem, the functions $\vec{f} \in [L^2(\Omega)]^2$ and $\vec{g} \in [L^2(\Gamma_N)]^2$ stand for the force per unit mass and the traction, respectively, while, with an abuse of notation, $\vec{v}_D \in [H^1(\Omega)]^2$ defines the extension into Ω of the actual Dirichlet datum $\vec{v}_D \in [H^{1/2}(\Gamma_D)]^2$. Finally \vec{n} stands for the unit outward normal vector to $\partial\Omega$.

System (32) represents the reference *strong form* for our a posteriori analysis. In particular we are referring to the conservative form (with respect to the stress rate $\boldsymbol{\sigma}$) of the incompressible Navier-Stokes equations, also accommodating possible nonhomogeneous Dirichlet conditions, typically prescribed at the inflow sections of the boundary.

In view of the weak form associated with (32), we first introduce the spaces $V = W = [H^1(\Omega)]^2 \times L^2(\Omega)$, $V_0 = W_0 = [H_{\Gamma_D}^1(\Omega)]^2 \times L^2(\Omega)$; then we split the velocity \vec{v} as $\vec{v} = \vec{v}_0 + \vec{v}_D$, with $\vec{v}_0 \in [H_{\Gamma_D}^1(\Omega)]^2$, while introducing the compact notation $U_D = (\vec{v}_D, 0) \in V$ such that $U = (\vec{v}, p) \in V_c \equiv U_D + V_0$. Thus the *weak form* corresponding to (32) is: find $U = U_D + (\vec{v}_0, p) \in V_c$, with $(\vec{v}_0, p) \in V_0$, such that

$$a(U)(\boldsymbol{\varphi}) = F(\boldsymbol{\varphi}) \quad \forall \boldsymbol{\varphi} = (\vec{\varphi}^v, \varphi^p) \in W_0, \quad (33)$$

where the semilinear and linear forms $a(\cdot)(\cdot)$ and $F(\cdot)$ are given by

$$\begin{aligned} a(U)(\boldsymbol{\varphi}) &= \int_{\Omega} 2\mu \boldsymbol{\epsilon}(\vec{v}) : \boldsymbol{\epsilon}(\vec{\varphi}^v) d\Omega + \int_{\Omega} (\vec{v} \cdot \nabla) \vec{v} \cdot \vec{\varphi}^v d\Omega \\ &\quad - \int_{\Omega} p \nabla \cdot \vec{\varphi}^v d\Omega + \int_{\Omega} \varphi^p \nabla \cdot \vec{v} d\Omega, \\ F(\boldsymbol{\varphi}) &= \int_{\Omega} \vec{f} \cdot \vec{\varphi}^v d\Omega + \int_{\Gamma_N} \vec{g} \cdot \vec{\varphi}^v ds, \end{aligned} \quad (34)$$

respectively. Problem (32) perfectly fits the general strong primal problem (9) after identifying U with the dummy unknown u , the operator $\mathcal{A}(u)$ and the source term f with

$$\mathcal{A}(U) = \begin{bmatrix} -\nabla \cdot \boldsymbol{\sigma}(\vec{v}, p) + (\vec{v} \cdot \nabla) \vec{v} \\ \nabla \cdot \vec{v} \end{bmatrix} \quad \text{and} \quad f = [\vec{f}, 0]^T,$$

respectively, and choosing as boundary conditions the mixed ones (32)₃-(32)₄. Likewise the weak form (33) conforms to the weak primal problem (10), upon choosing the spaces V, W, V_0 and W_0 as above, the quantity c linking the spaces V_c and V_0 as U_D , and the forms $a(\cdot)(\cdot)$ and $F(\cdot)$ as in (34).

Remark 4.1 *To guarantee the well-posedness of the weak form (33) in the case when $\Gamma_N = \emptyset$, the space V has to be replaced by the new one $V = [H^1(\Omega)]^2 \times L_0^2(\Omega)$, with $L_0^2(\Omega) = \{p \in L^2(\Omega) : \int_{\Omega} p d\Omega = 0\}$ (see, for instance, [19, 33]).*

Concerning the dual framework, it can be checked, via the identity (17), that the strong form of the adjoint Navier-Stokes equations is given by

$$\begin{cases} -\nabla \cdot \boldsymbol{\sigma}_A + (\nabla \vec{v})^T \vec{w} - (\nabla \cdot \vec{v}) \vec{w} - (\vec{v} \cdot \nabla) \vec{w} = \mathbf{j}_w & \text{in } \Omega, \\ -\nabla \cdot \vec{w} = j_r & \text{in } \Omega, \end{cases} \quad (35)$$

where $\boldsymbol{\sigma}_A = \boldsymbol{\sigma}_A(\vec{w}, r) = 2\mu \boldsymbol{\epsilon}(\vec{w}) + r\mathbf{I}$ is the adjoint stress rate depending on the *dual velocity* \vec{w} and on the *dual pressure* r . Identifying the dummy dual unknown z in (16) with $Z = (\vec{w}, r)$, we recover the strong form of the dual problem upon recognizing the operator $\mathcal{A}'(u)^*$ and the vector density j as

$$\mathcal{A}'(U)^* Z = \begin{bmatrix} -\nabla \cdot \boldsymbol{\sigma}_A(\vec{w}, r) + (\nabla \vec{v})^T \vec{w} - (\nabla \cdot \vec{v}) \vec{w} - (\vec{v} \cdot \nabla) \vec{w} \\ -\nabla \cdot \vec{w} \end{bmatrix}, \quad j = [j_w, j_r]^T.$$

We underline that the dual problem is always linear independently of the linear or nonlinear nature of the corresponding primal formulation. In particular in (35) three linear terms of the first order replace the nonlinear term $(\vec{v} \cdot \nabla) \vec{v}$ of the primal formulation.

Let us move to the dual boundary conditions issue. According to the theory in [13], we have that a dual Robin condition corresponds to a primal Neumann one, while primal Dirichlet conditions are preserved in the dual framework. In more detail we complete problem (35) with both nonhomogeneous Robin and Dirichlet boundary conditions

$$\boldsymbol{\sigma}_A \vec{n} + (\vec{v} \cdot \vec{n}) \vec{w} = \vec{q} \quad \text{on } \Gamma_N, \quad \vec{w} = \vec{w}_D \quad \text{on } \Gamma_D, \quad (36)$$

with $\vec{w}_D \in [H^1(\Omega)]^2$ the extension into Ω of the actual Dirichlet datum $\vec{w}_D \in [H^{1/2}(\Gamma_D)]^2$, and $\vec{q} \in [L^2(\Gamma_N)]^2$.

Before providing the weak form associated with the dual problem (35)-(36), let us split the velocity unknown as $\vec{w} = \vec{w}_D + \vec{w}_0$, with $\vec{w}_0 \in W_0$, W_0 being defined as above. Correspondingly, we introduce $Z_D = (\vec{w}_D, 0) \in W$ so that $W_d = Z_D + W_0$ and $Z = Z_D + (\vec{w}_0, r)$ is the actual dual unknown. The *weak form* corresponding to (35)-(36) is: find $Z = Z_D + (\vec{w}_0, r) \in W_d$, with $(\vec{w}_0, r) \in W_0$, such that

$$a'(U)(Z, \Psi) = J'(U)(\Psi) \quad \forall \Psi = (\vec{\psi}^w, \psi^r) \in V_0, \quad (37)$$

where $V_0 = W_0$, and

$$\begin{aligned}
a'(U)(Z, \Psi) &= \int_{\Omega} 2\mu \boldsymbol{\epsilon}(\vec{\psi}^w) : \boldsymbol{\epsilon}(\vec{w}) \, d\Omega + \int_{\Omega} (\vec{\psi}^w \cdot \nabla) \vec{v} \cdot \vec{w} \, d\Omega \\
&+ \int_{\Omega} (\vec{v} \cdot \nabla) \vec{\psi}^w \cdot \vec{w} \, d\Omega + \int_{\Omega} r \nabla \cdot \vec{\psi}^w \, d\Omega - \int_{\Omega} \psi^r \nabla \cdot \vec{w} \, d\Omega, \\
J'(U)(\Psi) &= \int_{\Omega} \mathbf{j}_w \cdot \vec{\psi}^w \, d\Omega + \int_{\Omega} j_r \psi^r \, d\Omega + \int_{\Gamma_N} \vec{q} \cdot \vec{\psi}^w \, ds.
\end{aligned} \tag{38}$$

Let us now deal with the discretization setting by introducing the finite dimensional counterparts of (33) and (37). They are easily obtained particularizing relations (21) to the problem at hand: find $(U_h, Z_h) \in V_{c,h} \times W_{d,h}$ such that

$$\begin{aligned}
a(U_h)(\boldsymbol{\varphi}_h) - \langle f - \mathcal{A}(U_h), \mathcal{S}_p(U_h)\boldsymbol{\varphi}_h \rangle_{\tau} &= F(\boldsymbol{\varphi}_h) \quad \forall \boldsymbol{\varphi}_h \in W_{0,h}, \\
a'(U_h)(Z_h, \Psi_h) - \langle j - \mathcal{A}'(U_h)^* Z_h, \mathcal{S}_d(U_h)\Psi_h \rangle_{\tau} &= J'(U_h)(\Psi_h) \quad \forall \Psi_h \in V_{0,h}.
\end{aligned} \tag{39}$$

With a view to the a posteriori analysis below and, in particular, of our interest into the anisotropic setting, we resort to a finite element approximation, thus identifying both the spaces $V_{0,h}$ and $W_{0,h}$ in (39) with $[Y_h \cap H_{\Gamma_D}^1(\Omega)]^2$, Y_h being the finite element space defined in § 2.2. In more detail we consider the discrete counterpart of the (weak) variables U and U_D represented by $U_h = (\vec{v}_h, p_h) \in Y_h^2 \times Y_h$, with $\vec{v}_h = \vec{v}_{D,h} + \vec{v}_{0,h}$ and $\vec{v}_{0,h} \in V_{0,h}$, and $U_{D,h} = (\vec{v}_{D,h}, 0) \in Y_h^2 \times Y_h$, respectively. Likewise for the dual variables: we let $Z_h = (\vec{w}_h, r_h) \in Y_h^2 \times Y_h$, with $\vec{w}_h = \vec{w}_{D,h} + \vec{w}_{0,h}$ and $\vec{w}_{0,h} \in W_{0,h}$, and $Z_{D,h} = (\vec{w}_{D,h}, 0) \in Y_h^2 \times Y_h$ as discrete counterparts of Z and Z_D . Notice that $\vec{v}_{D,h}, \vec{w}_{D,h} \in Y_h^2$ are proper finite element approximations of the extension of the Dirichlet data \vec{v}_D, \vec{w}_D , respectively, into Ω . Moreover, the quantities c_h, d_h approximating the data c, d , are thus identified with $U_{D,h}, Z_{D,h}$, respectively. To summarize the choices $V_{c,h} = U_{D,h} + V_{0,h}$ and $W_{d,h} = Z_{D,h} + W_{0,h}$ are made for the discrete spaces.

4.1 An anisotropic a posteriori error estimator for the Navier-Stokes equations

We are now in a position to merge the DWR “philosophy” of § 3 with the anisotropic setting provided into § 2.2. The resulting “machinery” is directly particularized to the Navier-Stokes system (32). With a view to the error estimate stemming from this compound analysis, let us anticipate some fundamental notation. For any $K \in \mathcal{T}_h$, we first introduce the primal $(\boldsymbol{\rho}_{1,p,K} = [\rho_{1,p,K}^1, \rho_{1,p,K}^2]^T$ and $\rho_{2,p,K}$) and the dual $(\boldsymbol{\rho}_{1,d,K} = [\rho_{1,d,K}^1, \rho_{1,d,K}^2]^T$ and $\rho_{2,d,K})$ *internal residuals* associated with the approximations U_h and Z_h , given by

$$\boldsymbol{\rho}_{1,p,K} = (\vec{f} + \nabla \cdot \boldsymbol{\sigma}(\vec{v}_h, p_h) - (\vec{v}_h \cdot \nabla) \vec{v}_h)|_K, \quad \rho_{2,p,K} = (-\nabla \cdot \vec{v}_h)|_K, \tag{40}$$

and

$$\begin{aligned}\boldsymbol{\rho}_{1,d,K} &= (\boldsymbol{j}_w + \nabla \cdot \boldsymbol{\sigma}_A(\bar{w}_h, r_h) - (\nabla \bar{v}_h)^T \bar{w}_h + (\nabla \cdot \bar{v}_h) \bar{w}_h + (\bar{v}_h \cdot \nabla) \bar{w}_h)|_K, \\ \rho_{2,d,K} &= (j_r + \nabla \cdot \bar{w}_h)|_K,\end{aligned}\tag{41}$$

respectively. We then define the primal and dual *boundary residuals*, identified by

$$\boldsymbol{j}_{p,e} = [j_{p,e}^1, j_{p,e}^2]^T = \begin{cases} -2\boldsymbol{\sigma}(\bar{v}_h, p_h)\bar{\boldsymbol{n}}_K|_e & \forall e \in \partial K \cap \mathcal{E}_{h,D}, \\ 2(\bar{q} - \boldsymbol{\sigma}(\bar{v}_h, p_h)\bar{\boldsymbol{n}}_K)|_e & \forall e \in \partial K \cap \mathcal{E}_{h,N}, \\ -[\boldsymbol{\sigma}(\bar{v}_h, p_h)\bar{\boldsymbol{n}}_K]_e & \forall e \in \partial K \cap \mathcal{E}_h^{int}, \end{cases}\tag{42}$$

and

$$\boldsymbol{j}_{d,e} = [j_{d,e}^1, j_{d,e}^2]^T = \begin{cases} -2(\boldsymbol{\sigma}_A(\bar{w}_h, r_h)\bar{\boldsymbol{n}}_K + (\bar{v}_h \cdot \bar{\boldsymbol{n}}_K) \bar{w}_h)|_e & \forall e \in \partial K \cap \mathcal{E}_{h,D}, \\ 2(\bar{q} - \boldsymbol{\sigma}_A(\bar{w}_h, r_h)\bar{\boldsymbol{n}}_K - (\bar{v}_h \cdot \bar{\boldsymbol{n}}_K) \bar{w}_h)|_e & \forall e \in \partial K \cap \mathcal{E}_{h,N}, \\ -[\boldsymbol{\sigma}_A(\bar{w}_h, r_h)\bar{\boldsymbol{n}}_K + (\bar{v}_h \cdot \bar{\boldsymbol{n}}_K) \bar{w}_h]_e & \forall e \in \partial K \cap \mathcal{E}_h^{int}, \end{cases}\tag{43}$$

respectively, where \mathcal{E}_h^{int} denotes the set of the internal edges of the skeleton \mathcal{E}_h of the triangulation \mathcal{T}_h , while $\mathcal{E}_{h,D}$ and $\mathcal{E}_{h,N}$ stands for the Dirichlet and Neumann subset of \mathcal{E}_h , respectively. Finally, with the notation $[v]_e$ we identify the standard jump function across the edge e given by

$$[v]_e(\vec{x}) = \lim_{\epsilon \rightarrow 0^+} v(\vec{x} + \epsilon \bar{\boldsymbol{n}}_e) - v(\vec{x} - \epsilon \bar{\boldsymbol{n}}_e), \quad \forall \vec{x} \in e,$$

with v any given real- or vector-valued function, and with $\bar{\boldsymbol{n}}_e$ any fixed unit outward normal vector to e .

The main result of this section is thus delivered via the following

Proposition 4.1 *Let U and Z be the solutions to the primal and to the dual problem (33) and (37), respectively, and let U_h and Z_h be the corresponding approximations, solutions to (39)₁ and (39)₂, respectively. Let $J(\cdot)$ be the functional of interest identifying the goal quantity $J(U)$. Then the following estimate holds*

$$|J(U) - J(U_h)| \leq C \sum_{i=1}^9 \eta_i,\tag{44}$$

where:

$$\eta_1 = \frac{1}{2} \sum_{K \in \mathcal{T}_h} (\boldsymbol{\rho}_{p,K} \cdot \boldsymbol{\omega}_{d,K} + \boldsymbol{\rho}_{d,K} \cdot \boldsymbol{\omega}_{p,K}),\tag{45}$$

with

$$\boldsymbol{\rho}_{p,K} \cdot \boldsymbol{\omega}_{d,K} = \sum_{j=1}^3 R_{p,K}^j \omega_{d,K}^j, \quad \boldsymbol{\rho}_{d,K} \cdot \boldsymbol{\omega}_{p,K} = \sum_{j=1}^3 R_{d,K}^j \omega_{p,K}^j,$$

where the “composite” primal and dual residuals $R_{p,K}^j$ and $R_{d,K}^j$, defined as

$$\begin{aligned} R_{p,K}^s &= \|\rho_{1,p,K}^s\|_{L^2(K)} + \frac{1}{2} \left(\frac{\lambda_{1,K}^2 + \lambda_{2,K}^2}{\lambda_{2,K}^3} \right)^{1/2} \|j_{p,e}^s\|_{L^2(\partial K)}, \quad R_{p,K}^3 = \|\rho_{2,p,K}\|_{L^2(K)}, \\ R_{d,K}^s &= \|\rho_{1,d,K}^s\|_{L^2(K)} + \frac{1}{2} \left(\frac{\lambda_{1,K}^2 + \lambda_{2,K}^2}{\lambda_{2,K}^3} \right)^{1/2} \|j_{d,e}^s\|_{L^2(\partial K)}, \quad R_{d,K}^3 = \|\rho_{2,d,K}\|_{L^2(K)}, \end{aligned}$$

for $s = 1, 2$, blend the information of the internal and boundary residuals (40)-(43), while the weights

$$\begin{aligned} \omega_{p,K}^s &= \left[\sum_{i,j=1}^2 \lambda_{i,K}^2 \lambda_{j,K}^2 L_K^{i,j}(e_{0,v}^s) \right]^{1/2}, \quad \omega_{p,K}^3 = \left[\sum_{i=1}^2 \lambda_{i,K}^2 (\vec{r}_{i,K}^T G_K(e_p) \vec{r}_{i,K}) \right]^{1/2}, \\ \omega_{d,K}^s &= \left[\sum_{i,j=1}^2 \lambda_{i,K}^2 \lambda_{j,K}^2 L_K^{i,j}(e_{0,w}^s) \right]^{1/2}, \quad \omega_{d,K}^3 = \left[\sum_{i=1}^2 \lambda_{i,K}^2 (\vec{r}_{i,K}^T G_K(e_r) \vec{r}_{i,K}) \right]^{1/2}. \end{aligned} \quad (46)$$

for $s = 1, 2$, collect the anisotropic information of the estimator, $\mathbf{e}_{0,v} = \vec{v}_0 - \vec{v}_{0,h} = [e_{0,v}^1, e_{0,v}^2]^T$ ($\mathbf{e}_{0,w} = \vec{w}_0 - \vec{w}_{0,h} = [e_{0,w}^1, e_{0,w}^2]^T$) being the “homogeneous” part of the primal (dual) velocity error $\mathbf{e}_v = \vec{v} - \vec{v}_h = [e_v^1, e_v^2]^T$ ($\mathbf{e}_w = \vec{w} - \vec{w}_h = [e_w^1, e_w^2]^T$), and with $e_p = p - p_h$ ($e_r = r - r_h$) the primal (dual) error associated with the pressure unknown;

$$\begin{aligned} \eta_2 &= \frac{1}{2} \sum_{K \in \mathcal{T}_h} \left[\int_K \boldsymbol{\rho}_{1,p,K} \cdot \mathbf{e}_{w_D} dK + \frac{1}{2} \int_{\partial K} \mathbf{j}_{p,e} \cdot \mathbf{e}_{w_D} ds \right], \\ \eta_3 &= \frac{1}{2} \sum_{K \in \mathcal{T}_h} \left[\int_K \boldsymbol{\rho}_{1,d,K} \cdot \mathbf{e}_{v_D} dK + \frac{1}{2} \int_{\partial K} \mathbf{j}_{d,e} \cdot \mathbf{e}_{v_D} ds \right], \end{aligned}$$

with $\mathbf{e}_{v_D} = \vec{v}_D - \vec{v}_{D,h}$ and $\mathbf{e}_{w_D} = \vec{w}_D - \vec{w}_{D,h}$ the errors related to the primal and dual data approximation, respectively;

$$\begin{aligned} \eta_4 &= -\frac{1}{2} \sum_{K \in \mathcal{T}_h} \tau_K \int_K \left\{ \boldsymbol{\rho}_{1,p,K} \cdot \mathbf{S}_p^1(\vec{v}_h, p_h) \Pi_h(\mathbf{e}_{0,w}) + \rho_{2,p,K} S_p^2(\vec{v}_h, p_h) I_h(e_r) \right. \\ &\quad \left. + \boldsymbol{\rho}_{1,d,K} \cdot \mathbf{S}_d^1(\vec{v}_h, p_h) \Pi_h(\mathbf{e}_{0,v}) + \rho_{2,d,K} S_d^2(\vec{v}_h, p_h) I_h(e_p) \right\} dK, \end{aligned}$$

with τ_K suitable stabilization parameters (to be defined later), Π_h and I_h the linear Lagrange and Clément interpolant introduced in § 2.2, and $\mathbf{S}_p = [\mathbf{S}_p^1, \mathbf{S}_p^2]^T$ and $\mathbf{S}_d = [\mathbf{S}_d^1, \mathbf{S}_d^2]^T$ the stabilization terms associated with the primal and the dual problem, respectively, according to the notation in (20);

$$\begin{aligned} \eta_5 &= \int_{\Omega} 2\mu \boldsymbol{\epsilon}(\mathbf{e}_v) : \boldsymbol{\epsilon}(\vec{w}_{D,h}) d\Omega - \int_{\Omega} e_p \nabla \cdot \vec{w}_{D,h} d\Omega + \int_{\Omega} [(\vec{v} \cdot \nabla) \vec{v} - (\vec{v}_h \cdot \nabla) \vec{v}_h] \cdot \vec{w}_{D,h} d\Omega; \\ \eta_6 &= \frac{1}{2} \left[\int_{\Omega} \left\{ 2\mu \boldsymbol{\epsilon}(\vec{v}) : \boldsymbol{\epsilon}(\mathbf{e}_{w_D}) + (\vec{v} \cdot \nabla) \vec{v} \cdot \mathbf{e}_{w_D} - p \nabla \cdot \mathbf{e}_{w_D} - \vec{f} \cdot \mathbf{e}_{w_D} \right\} d\Omega - \int_{\Gamma_N} \vec{g} \cdot \mathbf{e}_{w_D} ds \right]; \end{aligned}$$

$$\begin{aligned}
\eta_7 &= - \sum_{K \in \mathcal{T}_h} \tau_K \int_K \left\{ \boldsymbol{\rho}_{1,p,K} \cdot \mathbf{S}_p^1(\vec{v}_h, p_h) \vec{w}_{0,h} + \rho_{2,p,K} S_p^2(\vec{v}_h, p_h) r_h \right\} dK; \\
\eta_8 &= \frac{1}{2} \left[\int_{\Gamma_N} \vec{q} \cdot \mathbf{e}_{v_D} ds + \int_{\Omega} \left\{ \mathbf{j}_w \cdot \mathbf{e}_{v_D} - 2\mu \boldsymbol{\epsilon}(\mathbf{e}_{v_D}) : \boldsymbol{\epsilon}(\vec{w}) \right. \right. \\
&\quad \left. \left. - (\mathbf{e}_{v_D} \cdot \nabla) \vec{v} \cdot \vec{w} - (\vec{v} \cdot \nabla) \mathbf{e}_{v_D} \cdot \vec{w} - r \nabla \cdot \mathbf{e}_{v_D} \right\} d\Omega \right]; \\
\eta_9 &= \frac{1}{2} \left[\int_0^1 J'''(\{\vec{v}_h + s\mathbf{e}_v, p_h + s\mathbf{e}_p\})(\mathbf{E}_U, \mathbf{E}_U, \mathbf{E}_U) s(1-s) ds - \int_{\Omega} (\mathbf{e}_v \cdot \nabla) \mathbf{e}_v \cdot \mathbf{e}_w d\Omega \right]
\end{aligned}$$

still representing a third order remainder term in compliance with (27), with $\mathbf{E}_U = U - U_h = (\mathbf{e}_v, \mathbf{e}_p)$ the “global” primal error.

Proof. The thesis follows essentially from the abstract result of Proposition 3.3. In particular, we focus on the term I, by showing that it can be bounded by the quantity η_1 defined in (45). With this aim, we first exploit the definitions (29) of the weak residuals, while recalling that the primal and the dual error can be decomposed as $U - U_h = U_D - U_{D,h} + e_{0,U}$, $Z - Z_h = Z_D - Z_{D,h} + e_{0,Z}$, respectively, with $e_{0,U} = (\mathbf{e}_{0,v}, \mathbf{e}_p)^T \in V_0$ and $e_{0,Z} = (\mathbf{e}_{0,w}, e_r)^T \in W_0$. This yields

$$\begin{aligned}
\text{I} &= \frac{1}{2} [F((\mathcal{I} - \mathcal{P}_W)e_{0,Z}) - a(U_h)((\mathcal{I} - \mathcal{P}_W)e_{0,Z})] \\
&\quad + \frac{1}{2} [J'(U_h)((\mathcal{I} - \mathcal{P}_V)e_{0,U}) - a'(U_h)(Z_h, (\mathcal{I} - \mathcal{P}_V)e_{0,U})] = \text{I}_a + \text{I}_b,
\end{aligned}$$

\mathcal{I} denoting the identity operator and with \mathcal{P}_V and \mathcal{P}_W defined in terms of the Lagrange and Clément interpolant assigned in § 2.2, as $\mathcal{P}_V = \mathcal{P}_W = (\Pi_h, I_h)$. We deal now with I_a and I_b in turn, starting from the first term. We employ the definitions (34) identifying the primal formulation, to get

$$\begin{aligned}
\text{I}_a &= \frac{1}{2} \left[\int_{\Omega} \vec{f} \cdot ((\mathcal{I} - \Pi_h)\mathbf{e}_{0,w}) d\Omega + \int_{\Gamma_N} \vec{g} \cdot ((\mathcal{I} - \Pi_h)\mathbf{e}_{0,w}) ds \right. \\
&\quad \left. - \int_{\Omega} 2\mu \boldsymbol{\epsilon}(\vec{v}_h) : \boldsymbol{\epsilon}((\mathcal{I} - \Pi_h)\mathbf{e}_{0,w}) d\Omega - \int_{\Omega} (\vec{v}_h \cdot \nabla) \vec{v}_h \cdot ((\mathcal{I} - \Pi_h)\mathbf{e}_{0,w}) d\Omega \right. \\
&\quad \left. + \int_{\Omega} p_h \nabla \cdot ((\mathcal{I} - \Pi_h)\mathbf{e}_{0,w}) d\Omega - \int_{\Omega} ((\mathcal{I} - I_h)e_r) \nabla \cdot \vec{v}_h d\Omega \right]. \quad (47)
\end{aligned}$$

Now let us resort to a routine procedure in the context of a posteriori error estimator (see, for instance, [34]). In more detail we first split all the integrals in (47) using the identities $\int_{\Omega} \cdot d\Omega = \sum_{K \in \mathcal{T}_h} \int_K \cdot dK$ and $\int_{\Gamma_N} \cdot ds = \sum_{K \in \mathcal{T}_h} \int_{\partial K \cap \Gamma_N} \cdot ds$; then we integrate by parts the terms stemming from the third and fifth integrand in (47). After grouping the resulting terms, this yields

$$\begin{aligned}
\text{I}_a &= \frac{1}{2} \sum_{K \in \mathcal{T}_h} \left\{ \int_K \left[\vec{f} + \nabla \cdot \boldsymbol{\sigma}(\vec{v}_h, p_h) - (\vec{v}_h \cdot \nabla) \vec{v}_h \right] \cdot (\mathcal{I} - \Pi_h)\mathbf{e}_{0,w} dK \right. \\
&\quad \left. + \int_K (-\nabla \cdot \vec{v}_h)(\mathcal{I} - I_h)e_r dK - \int_{\partial K \cap \mathcal{E}_h^{\text{int}}} \boldsymbol{\sigma}(\vec{v}_h, p_h) \vec{n}_K \cdot (\mathcal{I} - \Pi_h)\mathbf{e}_{0,w} ds \right. \\
&\quad \left. - \int_{\partial K \cap \Gamma_D} \boldsymbol{\sigma}(\vec{v}_h, p_h) \vec{n}_K \cdot (\mathcal{I} - \Pi_h)\mathbf{e}_{0,w} ds \right. \\
&\quad \left. + \int_{\partial K \cap \Gamma_N} (\vec{g} - \boldsymbol{\sigma}(\vec{v}_h, p_h) \vec{n}_K) \cdot (\mathcal{I} - \Pi_h)\mathbf{e}_{0,w} ds \right\}. \quad (48)
\end{aligned}$$

Notice that the second boundary integral vanishes as $(\mathcal{I} - \Pi_h)\mathbf{e}_{0,w} = 0$ on Γ_D . However, since the boundary residual $\mathbf{j}_{p,e}$ on Γ_D plays a meaningful role in our final error estimator, we keep and involve it in the following even if aware of introducing a slight overestimation. On the other hand, the inclusion of this term could allow a reliable control of the data approximation if one took into account the quantities η_2 and η_3 for the purpose of mesh adaption.

Let us now address the dual contribution I_b : still using (29) combined with the definition of the dual forms (38), we obtain

$$\begin{aligned} I_b &= \frac{1}{2} \left[\int_{\Omega} \mathbf{j}_w \cdot (\mathcal{I} - \Pi_h)\mathbf{e}_{0,v} d\Omega + \int_{\Omega} j_r (\mathcal{I} - I_h)e_p d\Omega + \int_{\Gamma_N} \vec{q} \cdot (\mathcal{I} - \Pi_h)\mathbf{e}_{0,v} ds \right. \\ &\quad - \int_{\Omega} 2\mu \boldsymbol{\epsilon}((\mathcal{I} - \Pi_h)\mathbf{e}_{0,v}) : \boldsymbol{\epsilon}(\vec{w}_h) d\Omega - \int_{\Omega} ((\mathcal{I} - \Pi_h)\mathbf{e}_{0,v} \cdot \nabla) \vec{v}_h \cdot \vec{w}_h d\Omega \\ &\quad - \int_{\Omega} (\vec{v}_h \cdot \nabla) (\mathcal{I} - \Pi_h)\mathbf{e}_{0,v} \cdot \vec{w}_h d\Omega - \int_{\Omega} r_h \nabla \cdot (\mathcal{I} - \Pi_h)\mathbf{e}_{0,v} d\Omega \\ &\quad \left. + \int_{\Omega} (\mathcal{I} - I_h)e_p \nabla \cdot \vec{w}_h d\Omega \right]. \end{aligned}$$

Proceeding in an analogous fashion as for the primal contribution via a proper integration by parts, we obtain

$$\begin{aligned} I_b &= \frac{1}{2} \sum_{K \in \mathcal{T}_h} \left\{ \int_K \left[\mathbf{j}_w + \nabla \cdot \boldsymbol{\sigma}_A(\vec{w}_h, r_h) - (\nabla \vec{v}_h)^T \vec{w}_h + (\nabla \cdot \vec{v}_h) \vec{w}_h \right. \right. \\ &\quad \left. \left. + (\vec{v}_h \cdot \nabla) \vec{w}_h \right] \cdot (\mathcal{I} - \Pi_h)\mathbf{e}_{0,v} d\Omega + \int_K (j_r + \nabla \cdot \vec{w}_h)(\mathcal{I} - I_h)e_p d\Omega \right. \\ &\quad - \int_{\partial K \cap \mathcal{E}_h^{\text{int}}} \left[\boldsymbol{\sigma}_A(\vec{w}_h, r_h) \vec{n}_K + (\vec{v}_h \cdot \vec{n}_K) \vec{w}_h \right] \cdot (\mathcal{I} - \Pi_h)\mathbf{e}_{0,v} ds \\ &\quad + \int_{\partial K \cap \Gamma_N} \left[\vec{q} - \boldsymbol{\sigma}_A(\vec{w}_h, r_h) \vec{n}_K - (\vec{v}_h \cdot \vec{n}_K) \vec{w}_h \right] \cdot (\mathcal{I} - \Pi_h)\mathbf{e}_{0,v} ds \\ &\quad \left. - \int_{\partial K \cap \Gamma_D} \left[\boldsymbol{\sigma}_A(\vec{w}_h, r_h) \vec{n}_K + (\vec{v}_h \cdot \vec{n}_K) \vec{w}_h \right] \cdot (\mathcal{I} - \Pi_h)\mathbf{e}_{0,v} ds \right\}. \end{aligned} \quad (49)$$

Also in (49) we have a term, the last integral, vanishing and we still keep it in the analysis, exactly for the same reasons as above. In both (48) and (49), we now rewrite the integrals involving the interior edges using the property

$$\sum_{K \in \mathcal{T}_h} \int_{\partial K \cap \mathcal{E}_h^{\text{int}}} (\cdot) \vec{n}_K ds = \frac{1}{2} \sum_{K \in \mathcal{T}_h} \int_{\partial K \cap \mathcal{E}_h^{\text{int}}} [(\cdot) \vec{n}_K] ds,$$

$[\cdot]$ standing for the jump function. The anisotropic interpolation error estimates in Lemmas 2.1-2.2 are then applied. Finally the definitions (40)-(43) of the internal and boundary residuals deliver the estimator η_1 .

As for the terms η_2, η_3 , they are associated with the weak residuals II and III in (30), respectively. Their expression is obtained following the same steps as for the term I, but applied to the data errors $\vec{v}_D - \vec{v}_{D,h}$ and $\vec{w}_D - \vec{w}_{D,h}$. Note that in such a case the anisotropic error estimates are not exploited. As for the other terms in (44), $\eta_4 - \eta_9$, they are a straightforward translation of the terms IV-IX in (30). In particular, η_9 yields the expression of (27) for the Navier-Stokes equations, and this concludes the proof. \square

With a view to the actual numerical simulation, some remarks are in order, essentially as the structure of the terms constituting (44) is complex and all the quantities η_i , for $i = 1, \dots, 9$, are not explicitly computable, due to the dependence on the unknown primal and dual errors. To overcome this drawback, firstly we decided in favor of the computationally cheap option of implementing only the estimator η_1 and neglecting the other terms $\eta_i, i = 2, \dots, 9$. The rationale behind this choice is that we expect these latter to be of a higher order than η_1 , with respect to the mesh size. A rigorous justification of this statement, in an anisotropic context, is beyond the purpose of this paper, a corresponding a priori analysis being involved. In the isotropic case, an attempt in this direction is considered in [3]. Secondly, to make the estimator η_1 effective, in the spirit of what done in [26], we adopt the philosophy of the Zienkiewicz-Zhu gradient recovery procedure [35, 36]. In more detail, as the weights (46) depend on the first and second derivatives of the exact solution, we substitute these derivatives with suitably recovered ones, moving from the approximate solutions (\vec{v}_h, p_h) and (\vec{w}_h, r_h) . The actual implementation for the first derivatives is based on the area-weighted strategy of [29], while that for the second derivatives just relies on the already recovered first derivatives.

Remark 4.2 *Throughout the numerical computations we employ the GALs stabilization of [16] plus the anisotropic recipe for the parameters τ_K proposed in [27].*

5 The adaptive procedure

We employ, in a predictive fashion, a *metric-based* adaptive procedure exploiting the estimator η_1 in (45), embedded with the Zienkiewicz-Zhu recovery procedure.

Either of two different approaches are typically pursued in a mesh adaption framework:

- a) given a constraint on the maximum number of elements, find the mesh providing the most accurate numerical solution;
- b) given a constraint on the accuracy of the numerical solution, find the mesh with the least number of elements.

We here detail the approach b), while providing some comments on a) in Remark 5.1.

We recall that a metric is induced by a symmetric positive definite tensor field $\widetilde{M} : \Omega \rightarrow \mathbb{R}^{2 \times 2}$ (see, e.g., [17]). We first aim at clarifying the link existing between metric and mesh. With any given mesh \mathcal{T}_h , we can associate a piecewise constant metric $\widetilde{M}_{\mathcal{T}_h}$, such that, $\widetilde{M}_{\mathcal{T}_h}|_K = \widetilde{M}_K = B_K^{-2} = R_K^T \Lambda_K^{-2} R_K, \forall K \in \mathcal{T}_h$, the matrices R_K and Λ_K being the ones defined in § 2.2. With respect to this

metric, any triangle K of \mathcal{T}_h is unit equilateral, i.e.

$$\|e\|_{\widetilde{M}_{\mathcal{T}_h}} = \int_0^{|e|} \sqrt{\vec{t}^T \widetilde{M}_{\mathcal{T}_h}(s) \vec{t}} ds = 1,$$

with \vec{t} the unit tangent vector aligned with the generic edge e of K .

Suppose now that a metric \widetilde{M} is given. We show how an optimal mesh with respect to \widetilde{M} can be defined in terms of a so-called *matching condition*. With this respect, it is first of all convenient to diagonalize the tensor field \widetilde{M} as $\widetilde{M} = \widetilde{R}^T \widetilde{\Lambda}^{-2} \widetilde{R}$, with $\widetilde{\Lambda} = \text{diag}(\widetilde{\lambda}_1, \widetilde{\lambda}_2)$ and $\widetilde{R}^T = [\widetilde{r}_1, \widetilde{r}_2]$ positive diagonal and orthogonal matrices, respectively. For practical reasons, we approximate the quantities $\widetilde{\lambda}_1$, $\widetilde{\lambda}_2$, \widetilde{r}_1 and \widetilde{r}_2 identifying \widetilde{M} via functions piecewise constant over the triangulation \mathcal{T}_h , such that $\widetilde{r}_i|_K = \widetilde{r}_{i,K} \in \mathbb{R}^2$, $\widetilde{\lambda}_i|_K = \widetilde{\lambda}_{i,K} \in \mathbb{R}$, $\forall K \in \mathcal{T}_h$ and with $i = 1, 2$. We can thus introduce the *matching condition*:

Definition 5.1 *A mesh \mathcal{T}_h matches an assigned metric \widetilde{M} if, $\forall K \in \mathcal{T}_h$,*

$$\widetilde{M}|_K = \widetilde{M}_{\mathcal{T}_h}|_K, \quad (50)$$

i.e. $\widetilde{r}_{i,K} = \vec{r}_{i,K}$, $\widetilde{\lambda}_{i,K} = \lambda_{i,K}$, for $i = 1, 2$, the notation in § 2.2 being maintained.

We stress that in our case the tensor field \widetilde{M} is not explicitly given. Rather it must be obtained by solving the optimization problem b) reformulated with respect to the optimal metric (rather than the optimal mesh) in view of Definition 5.1.

The optimal metric turns out to be consequently our actual unknown.

In more detail, the computation of \widetilde{M} (and of the corresponding matching triangulation) is obtained via an iterative procedure: at each iteration, say j , we are dealing with three entities, namely the actual mesh $\mathcal{T}_h^{(j)}$, the new metric $\widetilde{M}^{(j+1)}$ computed on $\mathcal{T}_h^{(j)}$, and the updated mesh $\mathcal{T}_h^{(j+1)}$ matching $\widetilde{M}^{(j+1)}$. Both the problems (39) are first solved on $\mathcal{T}_h^{(j)}$. Then their solutions are used to set up suitable local optimization problems (one for each $K \in \mathcal{T}_h^{(j)}$), with the aim of identifying the metric $\widetilde{M}^{(j+1)}$ approximating the optimal metric \widetilde{M} , satisfying criterion b). Via the matching condition (50), the new mesh $\mathcal{T}_h^{(j+1)}$ is then built. This last task can be accomplished via proper metric-based mesh generators, such as, for instance, BAMG ([21]).

Let us now detail the local optimization procedure. We exemplify it on a typical term constituting the estimator η_1 represented by a product of the form $R_{p,K}^s \omega_{d,K}^s$ (or $R_{d,K}^s \omega_{p,K}^s$), for $s = 1, 2$. The term identified by the choice $s = 3$ will be separately managed. We aim at rewriting the term $R_{p,K}^s \omega_{d,K}^s$ as

$$R_{p,K}^s \omega_{d,K}^s = \alpha_{p,K}^s \widehat{R}_{p,K}^s \widehat{\omega}_{d,K}^s, \quad (51)$$

where $\alpha_{p,K}^s$ depends only on the area $|K|$ of K , $\widehat{R}_{p,K}^s$ is approximately a pointwise value (for a sufficiently fine mesh), while $\widehat{\omega}_{d,K}^s = \widehat{\omega}_{d,K}^s(\vec{r}_{1,K}, s_K)$ gathers the

anisotropic information (i.e. the stretching and the orientation) associated with K . In view of b) we first observe that minimizing the number of elements is equivalent to maximizing the area of each element. Thus as we are also interested in enforcing the equidistribution of the error by requiring that the term in (51) is equal to a local tolerance, say τ , $\forall K$, the only way to satisfy b) is to minimize $\widehat{\omega}_{d,K}^s$ with respect to $\vec{r}_{1,K}, s_K$. Then the values of $\lambda_{1,K}, \lambda_{2,K}$ are computed, via the equidistribution constraint, starting from the optimal value identified for s_K . Let us begin by recovering identity (51). Moving from (46) it suffices to make the following choices:

$$\begin{aligned}\alpha_{p,K}^s &= \frac{|K|^2}{|\widehat{K}|}, & \widehat{R}_{p,K}^s &= \frac{R_{p,K}^s}{|K|^{1/2}}, \\ \widehat{\omega}_{d,K}^s &= \left[s_K^2 \frac{L_K^{1,1}(e_{0,w}^s)}{|K|} + 2 \frac{L_K^{1,2}(e_{0,w}^s)}{|K|} + \frac{1}{s_K^2} \frac{L_K^{2,2}(e_{0,w}^s)}{|K|} \right]^{1/2},\end{aligned}\tag{52}$$

the relation $|K| = |\widehat{K}| \lambda_{1,K} \lambda_{2,K}$ having been exploited. We are now in a position to identify the following local constrained minimization:

$$\min_{s_K \geq 1, \vec{r}_{i,K} \cdot \vec{r}_{j,K} = \delta_{ij}} \widehat{\omega}_{d,K}^s(\vec{r}_{1,K}, s_K),\tag{53}$$

δ_{ij} being the Kronecker symbol and where it is understood that $\vec{r}_{1,K}$ and $\vec{r}_{2,K}$ are orthonormal vectors. The following statement provides us with the desired result:

Proposition 5.1 *Let the Hessian matrix $H_K(e_{0,w}^s)$ be constant over K and let $\{\vec{h}_{i,K}, h_{i,K}\}$ denote the eigenvector-eigenvalue pair of $H_K(e_{0,w}^s)/|K|^{1/2}$, with $|h_{1,K}| \geq |h_{2,K}| > 0$. Then the minimum (53) is reached for the choices*

$$\vec{r}_{1,K} = \vec{h}_{2,K} \quad \text{and} \quad s_K = \left| \frac{h_{1,K}}{h_{2,K}} \right|^{1/2},$$

and $\sqrt{2|h_{1,K}h_{2,K}|}$ is the minimum value thus attained by $\widehat{\omega}_{d,K}^s$.

The single values $\lambda_{1,K}, \lambda_{2,K}$ are then obtained by solving the two equations

$$\frac{|K|^2}{|\widehat{K}|} \widehat{R}_{p,K}^s \sqrt{2|h_{1,K}h_{2,K}|} = \tau \quad \text{and} \quad \frac{\lambda_{1,K}}{\lambda_{2,K}} = s_K = \left| \frac{h_{1,K}}{h_{2,K}} \right|^{1/2},\tag{54}$$

under the assumption that the dependence of $\widehat{R}_{p,K}^s$ on $\lambda_{1,K}, \lambda_{2,K}$ is treated explicitly, using the corresponding known values at the previous iterate. With simple algebraic manipulations we obtain from (54) the sought recipes for $\lambda_{1,K}$ and $\lambda_{2,K}$ given by

$$\lambda_{1,K} = \left(\frac{1}{\sqrt{2} |\widehat{K}| \widehat{R}_{p,K}^s} \left| \frac{h_{1,K}}{h_{2,K}^3} \right|^{1/2} \tau \right)^{1/4}, \quad \lambda_{2,K} = \left(\frac{1}{\sqrt{2} |\widehat{K}| \widehat{R}_{p,K}^s} \left| \frac{h_{2,K}}{h_{1,K}^3} \right|^{1/2} \tau \right)^{1/4}.$$

In the same spirit let us now deal with the term $R_{p,K}^3 \omega_{d,K}^3$ (or $R_{d,K}^3 \omega_{p,K}^3$). We rewrite it as

$$R_{p,K}^3 \omega_{d,K}^3 = \alpha_{p,K}^3 \widehat{R}_{p,K}^3 \widehat{\omega}_{d,K}^3, \quad (55)$$

where $\alpha_{p,K}^3 = \frac{|K|^{3/2}}{|\widehat{K}|^{1/2}}$, $\widehat{R}_{p,K}^3 = \frac{R_{p,K}^3}{|K|^{1/2}}$ and

$$\widehat{\omega}_{d,K}^3 = \left[s_K \left(\vec{r}_{1,K}^T \frac{G_K(e_r)}{|K|} \vec{r}_{1,K} \right) + \frac{1}{s_K} \left(\vec{r}_{2,K}^T \frac{G_K(e_r)}{|K|} \vec{r}_{2,K} \right) \right]^{1/2}.$$

The local constrained minimum we are looking for is

$$\min_{s_K \geq 1, \vec{r}_{i,K} \cdot \vec{r}_{j,K} = \delta_{ij}} \widehat{\omega}_{d,K}^3(\vec{r}_{1,K}, s_K), \quad (56)$$

with corresponding solution provided by the following

Proposition 5.2 *Let $\{\vec{g}_{i,K}, g_{i,K}\}$ be the eigenvector-eigenvalue pair of $G_K(e_r)/|K|$ with $g_{1,K} \geq g_{2,K} > 0$. Then the minimum (56) is identified by the choices*

$$\vec{r}_{1,K} = \vec{g}_{2,K} \quad \text{and} \quad s_K = \left(\frac{g_{1,K}}{g_{2,K}} \right)^{1/2},$$

yielding the value $(2\sqrt{g_{1,K}g_{2,K}})^{1/2}$ for $\widehat{\omega}_{d,K}^3$.

The corresponding optimal values for $\lambda_{1,K}, \lambda_{2,K}$ are finally obtained by solving the two equations

$$\frac{|K|^{3/2}}{|\widehat{K}|^{1/2}} \widehat{R}_{p,K}^3 (2\sqrt{g_{1,K}g_{2,K}})^{1/2} = \tau \quad \text{and} \quad \frac{\lambda_{1,K}}{\lambda_{2,K}} = s_K = \left(\frac{g_{1,K}}{g_{2,K}} \right)^{1/2} \quad (57)$$

still assuming that $\widehat{R}_{p,K}^3$ depends on the values $\lambda_{1,K}, \lambda_{2,K}$ at the previous iterate. System (57) provides us with the distinct values

$$\lambda_{1,K} = \left(\frac{1}{\sqrt{2}|\widehat{K}| \widehat{R}_{p,K}^3} \left(\frac{g_{1,K}}{g_{2,K}} \right)^{1/2} \tau \right)^{1/3}, \quad \lambda_{2,K} = \left(\frac{1}{\sqrt{2}|\widehat{K}| \widehat{R}_{p,K}^3} \left(\frac{g_{2,K}}{g_{1,K}} \right)^{1/2} \tau \right)^{1/3}.$$

Both the proofs of Propositions 5.1 and 5.2 are omitted for brevity.

By carrying out similar procedures for all the terms comprising the estimator η_1 in (45), we end up with a total of six metrics, three identified by the primal weights and three from the dual ones. The matter is now how to merge these six sources of anisotropic meshes in view of a single adapted anisotropic grid to contain the computational burden. We explain below how the six metrics can be combined into only two collecting the contributions due to the velocities and to the pressures, respectively. In such a case only two local optimization

problems need to be solved. In doing so, we aim at replacing η_1 with two new contributions, enjoying, at the same time, both reliability and the format (51). Then the new structure of the weights will still allow for an exact solution of the two corresponding minimization problems, similar to the ones tackled in Propositions 5.1 and 5.2. For this purpose, we rename the velocity and pressure contributions in (45) as

$$T_{v,K} = \sum_{s=1}^2 \left\{ R_{p,K}^s \omega_{d,K}^s + R_{d,K}^s \omega_{p,K}^s \right\} \quad \text{and} \quad T_{p,K} = R_{p,K}^3 \omega_{d,K}^3 + R_{d,K}^3 \omega_{p,K}^3, \quad \forall K \in \mathcal{T}_h. \quad (58)$$

The next result can thus be stated:

Proposition 5.3 *The velocity and pressure contributions $T_{v,K}$ and $T_{p,K}$ in (58) can be bounded as*

$$T_{v,K} \leq 2 \alpha_{v,K} \widehat{\omega}_{v,K}, \quad T_{p,K} \leq \sqrt{2} \alpha_{p,K} \widehat{\omega}_{p,K}, \quad (59)$$

where:

$$\alpha_{v,K} = \frac{|K|^2}{|\widehat{K}|}; \quad \widehat{\omega}_{v,K} = \left[s_K^2 \frac{L_{v,K}^{1,1}}{|K|} + 2 \frac{L_{v,K}^{1,2}}{|K|} + \frac{1}{s_K^2} \frac{L_{v,K}^{2,2}}{|K|} \right]^{1/2}, \quad (60)$$

with

$$L_{v,K}^{i,j} = \int_K \left(\vec{r}_{i,K}^T \left[\sum_{s=1}^2 (\widehat{R}_{p,K}^s |H_K(e_{0,w}^s)| + \widehat{R}_{d,K}^s |H_K(e_{0,v}^s)|) \right] \vec{r}_{j,K} \right)^2 dK, \quad \text{for } i, j = 1, 2, \quad (61)$$

the symbol $|\cdot|$ denoting now the modulus matrix, and with $\widehat{R}_{p,K}^s$ ($\widehat{R}_{d,K}^s$) defined according to (52), for $s = 1, 2$;

$$\alpha_{p,K} = \frac{|K|^{3/2}}{|\widehat{K}|^{1/2}}; \quad \widehat{\omega}_{p,K} = \left[s_K \left(\vec{r}_{1,K}^T \frac{G_{p,K}}{|K|} \vec{r}_{1,K} \right) + \frac{1}{s_K} \left(\vec{r}_{2,K}^T \frac{G_{p,K}}{|K|} \vec{r}_{2,K} \right) \right]^{1/2},$$

the matrix $G_{p,K}$ being defined by

$$G_{p,K} = (\widehat{R}_{p,K}^3)^2 G_K(e_r) + (\widehat{R}_{d,K}^3)^2 G_K(e_p),$$

with $\widehat{R}_{p,K}^3$ ($\widehat{R}_{d,K}^3$) as in (55).

Notice that the quantities $L_{v,K}^{i,j}$ in (61) enjoy the same form as (1), the Hessian $H(v)$ being now replaced by the average

$$\sum_{s=1}^2 (\widehat{R}_{p,K}^s |H_K(e_w^s)| + \widehat{R}_{d,K}^s |H_K(e_v^s)|)$$

of the Hessian matrices associated with the primal and dual errors, each weighted by the complementary residual. The matrix $G_{p,K}$ averages in a similar way both primal ($G_K(e_p)$) and dual ($G_K(e_r)$) contributions. Moreover also the new weights $\widehat{\omega}_{v,K}$ and $\widehat{\omega}_{p,K}$ preserve the same structure as the corresponding ones $\widehat{\omega}_{p,K}^s$ and $\widehat{\omega}_{d,K}^s$, with $s = 1, 2$ in the case of the velocity contribution and $s = 3$ for the pressure.

The proof of Proposition 5.3 requires two preliminary Lemmas.

Lemma 5.1 *Let $A = Q \Lambda Q^T \in \mathbb{R}^{2 \times 2}$ be a symmetric matrix, with Q and $\Lambda = \text{diag}(\lambda_{1,A}, \lambda_{2,A})$ the orthogonal and the diagonal factor, respectively. Then it holds*

$$\begin{aligned} & s_K^2 (\vec{r}_{1,K}^T A \vec{r}_{1,K})^2 + 2 (\vec{r}_{1,K}^T A \vec{r}_{2,K})^2 + s_K^{-2} (\vec{r}_{2,K}^T A \vec{r}_{2,K})^2 \\ & \leq s_K^2 (\vec{r}_{1,K}^T |A| \vec{r}_{1,K})^2 + 2 (\vec{r}_{1,K}^T |A| \vec{r}_{2,K})^2 + s_K^{-2} (\vec{r}_{2,K}^T |A| \vec{r}_{2,K})^2, \end{aligned} \quad (62)$$

where $|A| = Q|\Lambda|Q^T$ is the modulus matrix of A , with $|\Lambda| = \text{diag}(|\lambda_{1,A}|, |\lambda_{2,A}|)$.

Proof. The thesis is equivalent to proving that $\|A\|_F \leq \|\bar{A}\|_F$, with $\|\cdot\|_F$ the Frobenius norm of a matrix, where

$$A = \begin{bmatrix} s_K \vec{r}_{1,K}^T A \vec{r}_{1,K} & \vec{r}_{1,K}^T A \vec{r}_{2,K} \\ \vec{r}_{1,K}^T A \vec{r}_{2,K} & s_K^{-1} \vec{r}_{2,K}^T A \vec{r}_{2,K} \end{bmatrix}, \quad \bar{A} = \begin{bmatrix} s_K \vec{r}_{1,K}^T |A| \vec{r}_{1,K} & \vec{r}_{1,K}^T |A| \vec{r}_{2,K} \\ \vec{r}_{1,K}^T |A| \vec{r}_{2,K} & s_K^{-1} \vec{r}_{2,K}^T |A| \vec{r}_{2,K} \end{bmatrix}.$$

Moreover, it suffices to consider a diagonal matrix A . Indeed, we have

$$\vec{r}_{i,K}^T A \vec{r}_{j,K} = \vec{r}_{i,K}^T Q \Lambda Q^T \vec{r}_{j,K} = \vec{q}_{i,K}^T \Lambda \vec{q}_{j,K},$$

with $\vec{q}_{i,K} = Q^T \vec{r}_{i,K}$, and $\vec{q}_{i,K} \cdot \vec{q}_{j,K} = \delta_{ij}$. Thus the $\vec{q}_{i,K}$'s can replace the $\vec{r}_{i,K}$'s which are orthonormalized too. Then let $\vec{q}_{1,K} = [\cos \theta, \sin \theta]^T$ and $\vec{q}_{2,K} = [-\sin \theta, \cos \theta]^T$, with $0 \leq \theta < \pi$. A straightforward calculation shows that

$$\begin{aligned} A &= \begin{bmatrix} s_K (\lambda_{1,A} \cos^2 \theta + \lambda_{2,A} \sin^2 \theta) & (\lambda_{2,A} - \lambda_{1,A}) \cos \theta \sin \theta \\ (\lambda_{2,A} - \lambda_{1,A}) \cos \theta \sin \theta & s_K^{-1} (\lambda_{1,A} \sin^2 \theta + \lambda_{2,A} \cos^2 \theta) \end{bmatrix}, \\ \bar{A} &= \begin{bmatrix} s_K (|\lambda_{1,A}| \cos^2 \theta + |\lambda_{2,A}| \sin^2 \theta) & (|\lambda_{2,A}| - |\lambda_{1,A}|) \cos \theta \sin \theta \\ (|\lambda_{2,A}| - |\lambda_{1,A}|) \cos \theta \sin \theta & s_K^{-1} (|\lambda_{1,A}| \sin^2 \theta + |\lambda_{2,A}| \cos^2 \theta) \end{bmatrix} \end{aligned}$$

and

$$\|\bar{A}\|_F - \|A\|_F = 2 (|\lambda_{1,A} \lambda_{2,A}| - \lambda_{1,A} \lambda_{2,A}) (s_K - s_K^{-1})^2 \cos^2 \theta \sin^2 \theta \geq 0.$$

This concludes the proof. \square

Lemma 5.2 *Let $A, B \in \mathbb{R}^{2 \times 2}$ be symmetric matrices. Then the following relation can be proved:*

$$\begin{aligned} & s_K^2 [(\vec{r}_{1,K}^T |A| \vec{r}_{1,K})^2 + (\vec{r}_{1,K}^T |B| \vec{r}_{1,K})^2] + 2 [(\vec{r}_{1,K}^T |A| \vec{r}_{2,K})^2 + (\vec{r}_{1,K}^T |B| \vec{r}_{2,K})^2] \\ & + s_K^{-2} [(\vec{r}_{2,K}^T |A| \vec{r}_{2,K})^2 + (\vec{r}_{2,K}^T |B| \vec{r}_{2,K})^2] \leq s_K^2 [\vec{r}_{1,K}^T (|A| + |B|) \vec{r}_{1,K}]^2 \\ & + 2 [\vec{r}_{1,K}^T (|A| + |B|) \vec{r}_{2,K}]^2 + s_K^{-2} [\vec{r}_{2,K}^T (|A| + |B|) \vec{r}_{2,K}]^2, \end{aligned} \quad (63)$$

$|A|$ and $|B|$ coinciding with the modulus matrices of A and B , respectively.

Proof. The assertion amounts to proving that $\|\bar{\mathcal{A}}\|_{\mathbb{F}}^2 + \|\bar{\mathcal{B}}\|_{\mathbb{F}}^2 \leq \|\bar{\mathcal{A}} + \bar{\mathcal{B}}\|_{\mathbb{F}}^2$, if we make the identifications

$$\bar{\mathcal{A}} = \begin{bmatrix} s_K \bar{r}_{1,K}^T |A| \bar{r}_{1,K} & \bar{r}_{1,K}^T |A| \bar{r}_{2,K} \\ \bar{r}_{1,K}^T |A| \bar{r}_{2,K} & s_K^{-1} \bar{r}_{2,K}^T |A| \bar{r}_{2,K} \end{bmatrix}, \quad \bar{\mathcal{B}} = \begin{bmatrix} s_K \bar{r}_{1,K}^T |B| \bar{r}_{1,K} & \bar{r}_{1,K}^T |B| \bar{r}_{2,K} \\ \bar{r}_{1,K}^T |B| \bar{r}_{2,K} & s_K^{-1} \bar{r}_{2,K}^T |B| \bar{r}_{2,K} \end{bmatrix}.$$

Using the definition of the Frobenius norm, we first observe that

$$\begin{aligned} \|\bar{\mathcal{A}} + \bar{\mathcal{B}}\|_{\mathbb{F}}^2 - \|\bar{\mathcal{A}}\|_{\mathbb{F}}^2 - \|\bar{\mathcal{B}}\|_{\mathbb{F}}^2 &= 2 [s_K^2 (\bar{r}_{1,K}^T |A| \bar{r}_{1,K}) (\bar{r}_{1,K}^T |B| \bar{r}_{1,K}) \\ &+ 2 (\bar{r}_{1,K}^T |A| \bar{r}_{2,K}) (\bar{r}_{1,K}^T |B| \bar{r}_{2,K}) + s_K^{-2} (\bar{r}_{2,K}^T |A| \bar{r}_{2,K}) (\bar{r}_{2,K}^T |B| \bar{r}_{2,K})] = 2 \bar{\mathcal{A}} : \bar{\mathcal{B}}, \end{aligned}$$

where $\bar{\mathcal{A}} : \bar{\mathcal{B}} = \sum_{i,j=1}^2 \bar{\mathcal{A}}_{ij} \bar{\mathcal{B}}_{ij}$ is the tensor scalar product. We then prove that both $\bar{\mathcal{A}}, \bar{\mathcal{B}}$ are symmetric and positive semi-definite. We check this only for $\bar{\mathcal{A}}$, the proof for $\bar{\mathcal{B}}$ being analogous. The symmetry of $\bar{\mathcal{A}}$ trivially holds. To verify the positive semi-definiteness, we prove that $\bar{\mathcal{A}}_{11} \geq 0, \det \bar{\mathcal{A}} \geq 0$. For this purpose, let $\bar{r}_{1,K} = [\cos \theta, \sin \theta]^T$ and $\bar{r}_{2,K} = [-\sin \theta, \cos \theta]^T$, with $0 \leq \theta < \pi$. Moreover, as in the proof of Lemma 5.1, it suffices to consider a diagonal matrix A . Then we have,

$$\bar{\mathcal{A}}_{11} = s_K (\bar{r}_{1,K}^T |A| \bar{r}_{1,K}) = s_K (|\lambda_{1,A}| \cos^2 \theta + |\lambda_{2,A}| \sin^2 \theta) \geq 0,$$

and

$$\begin{aligned} \det \bar{\mathcal{A}} &= (|\lambda_{1,A}| \cos^2 \theta + |\lambda_{2,A}| \sin^2 \theta) (|\lambda_{1,A}| \sin^2 \theta + |\lambda_{2,A}| \cos^2 \theta) \\ &- [\cos \theta \sin \theta (|\lambda_{2,A}| - |\lambda_{1,A}|)]^2 = |\lambda_{1,A}| |\lambda_{2,A}| (\cos^2 \theta + \sin^2 \theta)^2 = |\lambda_{1,A}| |\lambda_{2,A}| \geq 0. \end{aligned}$$

Thus, thanks to the positive semi-definiteness, it holds also $\bar{\mathcal{A}}_{22} \geq 0, \bar{\mathcal{B}}_{22} \geq 0$, and $|\bar{\mathcal{A}}_{12}| \leq \sqrt{\bar{\mathcal{A}}_{11} \bar{\mathcal{A}}_{22}}, |\bar{\mathcal{B}}_{12}| \leq \sqrt{\bar{\mathcal{B}}_{11} \bar{\mathcal{B}}_{22}}$. It follows that

$$\begin{aligned} \|\bar{\mathcal{A}} + \bar{\mathcal{B}}\|_{\mathbb{F}}^2 - \|\bar{\mathcal{A}}\|_{\mathbb{F}}^2 - \|\bar{\mathcal{B}}\|_{\mathbb{F}}^2 &= 2 \bar{\mathcal{A}} : \bar{\mathcal{B}} = 2 (\bar{\mathcal{A}}_{11} \bar{\mathcal{B}}_{11} + 2 \bar{\mathcal{A}}_{12} \bar{\mathcal{B}}_{12} + \bar{\mathcal{A}}_{22} \bar{\mathcal{B}}_{22}) \\ &\geq 2 (\bar{\mathcal{A}}_{11} \bar{\mathcal{B}}_{11} + \bar{\mathcal{A}}_{22} \bar{\mathcal{B}}_{22} - 2 \sqrt{\bar{\mathcal{A}}_{11} \bar{\mathcal{A}}_{22}} \sqrt{\bar{\mathcal{B}}_{11} \bar{\mathcal{B}}_{22}}) = 2 (\sqrt{\bar{\mathcal{A}}_{11} \bar{\mathcal{B}}_{11}} - \sqrt{\bar{\mathcal{A}}_{22} \bar{\mathcal{B}}_{22}})^2 \geq 0, \end{aligned}$$

and this ends the proof. \square

Result (63) can be easily generalized by induction to the case of n symmetric matrices. We can now close Proposition 5.3. **Proof.** Let us first consider the velocity term $T_{v,K}$. Moving from identity (51), we can write that

$$T_{v,K} = \sum_{s=1}^2 \left\{ R_{p,K}^s \omega_{d,K}^s + R_{d,K}^s \omega_{p,K}^s \right\} = \alpha_{v,K} \sum_{s=1}^2 \left\{ \hat{R}_{p,K}^s \hat{\omega}_{d,K}^s + \hat{R}_{d,K}^s \hat{\omega}_{p,K}^s \right\}, \quad (64)$$

where $\alpha_{v,K} = \alpha_{p,K}^s = \alpha_{d,K}^s = |K|^2 / |\hat{K}|$ according to (52). Now, using the property

$$\left(\sum_{i=1}^n a_i^2 \right)^{1/2} \leq \sum_{i=1}^n a_i \leq \sqrt{n} \left(\sum_{i=1}^n a_i^2 \right)^{1/2} \quad \forall n \in \mathbb{N} \quad (65)$$

and with $a_i \geq 0, \forall i = 1, \dots, n$, we can bound (64) as

$$T_{v,K} \leq 2 \alpha_{v,K} \left[\sum_{s=1}^2 \left\{ (\hat{R}_{p,K}^s \hat{\omega}_{d,K}^s)^2 + (\hat{R}_{d,K}^s \hat{\omega}_{p,K}^s)^2 \right\} \right]^{1/2}. \quad (66)$$

Via (52), let us now rewrite the right-hand side of (66) by expanding the definition of the weights $\widehat{\omega}_{p,K}^s, \widehat{\omega}_{d,K}^s$ as

$$\begin{aligned} T_{v,K} &\leq 2\alpha_{v,K} \left[\sum_{s=1}^2 \left\{ \frac{s_K^2}{|K|} \left[(\widehat{R}_{p,K}^s)^2 L_K^{1,1}(e_{0,w}^s) + (\widehat{R}_{d,K}^s)^2 L_K^{1,1}(e_{0,v}^s) \right] \right. \right. \\ &\quad + \frac{2}{|K|} \left[(\widehat{R}_{p,K}^s)^2 L_K^{1,2}(e_{0,w}^s) + (\widehat{R}_{d,K}^s)^2 L_K^{1,2}(e_{0,v}^s) \right] \\ &\quad \left. \left. + \frac{1}{s_K^2} \frac{1}{|K|} \left[(\widehat{R}_{p,K}^s)^2 L_K^{2,2}(e_{0,w}^s) + (\widehat{R}_{d,K}^s)^2 L_K^{2,2}(e_{0,v}^s) \right] \right\} \right]^{1/2}, \end{aligned}$$

i.e., using (1), as

$$\begin{aligned} T_{v,K} &\leq 2\alpha_{v,K} \left[\sum_{s=1}^2 \int_K \left\{ \frac{s_K^2}{|K|} \left[(\vec{r}_{1,K}^T \widehat{R}_{p,K}^s H_K(e_{0,w}^s) \vec{r}_{1,K})^2 + (\vec{r}_{1,K}^T \widehat{R}_{d,K}^s H_K(e_{0,v}^s) \vec{r}_{1,K})^2 \right] \right. \right. \\ &\quad + \frac{2}{|K|} \left[(\vec{r}_{1,K}^T \widehat{R}_{p,K}^s H_K(e_{0,w}^s) \vec{r}_{2,K})^2 + (\vec{r}_{1,K}^T \widehat{R}_{d,K}^s H_K(e_{0,v}^s) \vec{r}_{2,K})^2 \right] \\ &\quad \left. \left. + \frac{1}{s_K^2} \frac{1}{|K|} \left[(\vec{r}_{2,K}^T \widehat{R}_{p,K}^s H_K(e_{0,w}^s) \vec{r}_{2,K})^2 + (\vec{r}_{2,K}^T \widehat{R}_{d,K}^s H_K(e_{0,v}^s) \vec{r}_{2,K})^2 \right] \right\} dK \right]^{1/2}. \end{aligned} \tag{67}$$

The corresponding estimate in (59) now easily follows by properly applying to (67) Lemma 5.1 and the generalization of Lemma 5.2 to the case of four matrices. In more detail let us focus on what's up to the term associated with the factor $s_K^2/|K|$: from Lemma 5.1 used by identifying the matrix A in (62) in turn with the matrices $\widehat{R}_{p,K}^1 H_K(e_{0,w}^1), \widehat{R}_{p,K}^2 H_K(e_{0,w}^2), \widehat{R}_{d,K}^1 H_K(e_{0,v}^1), \widehat{R}_{d,K}^2 H_K(e_{0,v}^2)$, we first get

$$\begin{aligned} &\int_K \left[(\vec{r}_{1,K}^T \widehat{R}_{p,K}^1 H_K(e_{0,w}^1) \vec{r}_{1,K})^2 + (\vec{r}_{1,K}^T \widehat{R}_{d,K}^1 H_K(e_{0,v}^1) \vec{r}_{1,K})^2 \right. \\ &\quad \left. + (\vec{r}_{1,K}^T \widehat{R}_{p,K}^2 H_K(e_{0,w}^2) \vec{r}_{1,K})^2 + (\vec{r}_{1,K}^T \widehat{R}_{d,K}^2 H_K(e_{0,v}^2) \vec{r}_{1,K})^2 \right] dK \\ &\leq \int_K \left[(\vec{r}_{1,K}^T \widehat{R}_{p,K}^1 |H_K(e_{0,w}^1)| \vec{r}_{1,K})^2 + (\vec{r}_{1,K}^T \widehat{R}_{d,K}^1 |H_K(e_{0,v}^1)| \vec{r}_{1,K})^2 \right. \\ &\quad \left. + (\vec{r}_{1,K}^T \widehat{R}_{p,K}^2 |H_K(e_{0,w}^2)| \vec{r}_{1,K})^2 + (\vec{r}_{1,K}^T \widehat{R}_{d,K}^2 |H_K(e_{0,v}^2)| \vec{r}_{1,K})^2 \right] dK. \end{aligned}$$

Then we employ the extension of Lemma 5.2 to the four matrices $A = \widehat{R}_{p,K}^1 H_K(e_{0,w}^1), B = \widehat{R}_{d,K}^1 H_K(e_{0,v}^1), C = \widehat{R}_{p,K}^2 H_K(e_{0,w}^2), D = \widehat{R}_{d,K}^2 H_K(e_{0,v}^2)$, yielding

$$\begin{aligned} &\int_K \left[(\vec{r}_{1,K}^T \widehat{R}_{p,K}^1 H_K(e_{0,w}^1) \vec{r}_{1,K})^2 + (\vec{r}_{1,K}^T \widehat{R}_{d,K}^1 H_K(e_{0,v}^1) \vec{r}_{1,K})^2 \right. \\ &\quad \left. + (\vec{r}_{1,K}^T \widehat{R}_{p,K}^2 H_K(e_{0,w}^2) \vec{r}_{1,K})^2 + (\vec{r}_{1,K}^T \widehat{R}_{d,K}^2 H_K(e_{0,v}^2) \vec{r}_{1,K})^2 \right] dK \\ &\leq \int_K \left[\vec{r}_{1,K}^T \left(\widehat{R}_{p,K}^1 |H_K(e_{0,w}^1)| + \widehat{R}_{d,K}^1 |H_K(e_{0,v}^1)| \right. \right. \\ &\quad \left. \left. + \widehat{R}_{p,K}^2 |H_K(e_{0,w}^2)| + \widehat{R}_{d,K}^2 |H_K(e_{0,v}^2)| \right) \vec{r}_{1,K} \right]^2 dK, \end{aligned}$$

i.e., the corresponding term $L_{v,K}^{1,1}$ in (60) according to the definition (61).

After analyzing the terms related to the primal and dual velocities, let us consider the

pressure-dependent ones. Thanks to (55) we first have

$$T_{p,K} = R_{p,K}^3 \omega_{d,K}^3 + R_{d,K}^3 \omega_{p,K}^3 = \alpha_{p,K} (\widehat{R}_{p,K}^3 \widehat{\omega}_{d,K}^3 + \widehat{R}_{d,K}^3 \widehat{\omega}_{p,K}^3), \quad (68)$$

with $\alpha_{p,K} = \alpha_{p,K}^3 = \alpha_{d,K}^3 = |K|^{3/2}/|\widehat{K}|^{1/2}$. The right-hand side of (68) can be rewritten taking advantage from the definition of the weights $\widehat{\omega}_{p,K}^3, \widehat{\omega}_{d,K}^3$ as

$$\begin{aligned} T_{p,K} &= \alpha_{p,K} \left[s_K \left(\vec{r}_{1,K}^T (\widehat{R}_{p,K}^3)^2 \frac{G_K(e_r)}{|K|} \vec{r}_{1,K} \right) + \frac{1}{s_K} \left(\vec{r}_{2,K}^T (\widehat{R}_{p,K}^3)^2 \frac{G_K(e_r)}{|K|} \vec{r}_{2,K} \right) \right]^{1/2} \\ &+ \left[s_K \left(\vec{r}_{1,K}^T (\widehat{R}_{d,K}^3)^2 \frac{G_K(e_p)}{|K|} \vec{r}_{1,K} \right) + \frac{1}{s_K} \left(\vec{r}_{2,K}^T (\widehat{R}_{d,K}^3)^2 \frac{G_K(e_p)}{|K|} \vec{r}_{2,K} \right) \right]^{1/2}, \end{aligned}$$

and, using (65) yields the corresponding estimate in (59). \square

Proposition 5.3 thus allows us to manage just two metrics rather than the six ones identified by the estimator η_1 in (45). Likewise we are led to solve just two local optimization problems in the same spirit as Proposition 5.1 and 5.2, respectively. The only slight difference is the presence of the residuals into the weights in the case of (59) rather than as a factor multiplying the weight itself as in (51) or (55). This impasse is overcome simply by introducing a fictitious residual identically equal to 1 in (59).

To summarize, the adaptive algorithm used in practice reads:

Algorithm 5.1 Set $j = 0$:

1. build the background mesh $\mathcal{T}_h^{(j)}$;
2. solve the primal and dual problems (39);
3. solve the local minimization problems involving $\widehat{\omega}_{v,K}$ and $\widehat{\omega}_{p,K}$ for the pairs $(\widetilde{s}_{v,K}, \widetilde{r}_{1,v,K})$ and $(\widetilde{s}_{p,K}, \widetilde{r}_{1,p,K})$, respectively;
4. via the equidistribution principle, compute $(\widetilde{\lambda}_{1,v,K}, \widetilde{\lambda}_{2,v,K})$ and $(\widetilde{\lambda}_{1,p,K}, \widetilde{\lambda}_{2,p,K})$ starting from the optimal values $\widetilde{s}_{v,K}, \widetilde{s}_{p,K}$, respectively;
5. build up the new metrics $\widetilde{M}_v^{(j+1)}$ and $\widetilde{M}_p^{(j+1)}$;
6. construct the new mesh $\mathcal{T}_h^{(j+1)}$ matching either of the two metrics or a suitable intersection of them;
7. if a suitable stopping criterion is met, exit; else $j \leftarrow j + 1$ and go to 2.

For the concept of metric intersection we refer, for instance, to [17].

Remark 5.1 *If one is interested in the approach a) stated at the beginning of the section, the above adaptive procedure can be recycled except for the choice of the tolerance τ , now depending on the desired number of elements.*

6 Numerical results

For the purpose of validating the overall adaptive procedure itemized in the ALGORITHM 5.1, we report some numerical test cases.

6.1 The Brenner & Scott test case

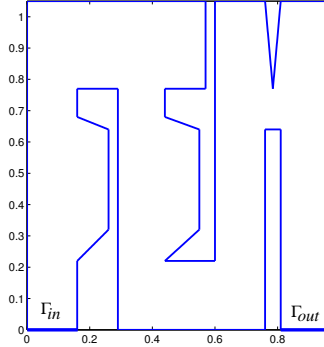


Figure 2: Domain Ω for the Brenner & Scott test case.

Let us identify the computational domain Ω with the one sketched in Figure 2. It models a FEM-shaped channel, and it is faithfully inspired by the Brenner & Scott's book cover [6]. Full Dirichlet boundary conditions are assigned on $\partial\Omega$: in particular, we choose

$$\begin{aligned} \vec{v} &= \frac{10^3}{6.4} (0, x_1 (0.16 - x_1))^T \quad \text{on} \quad \Gamma_{in} = \{x_2 = 0\} \cap \{0 < x_1 < 0.16\}, \\ \vec{v} &= \frac{10^3}{6.4} (0, (0.81 - x_1)(0.97 - x_1))^T \quad \text{on} \quad \Gamma_{out} = \{x_2 = 0\} \cap \{0.81 < x_1 < 0.97\}, \\ \vec{v} &= \vec{0} \quad \text{elsewhere,} \end{aligned}$$

Γ_{in} and Γ_{out} representing the inflow and the outflow section, respectively (see Figure 2). Finally, the kinematic viscosity μ is set equal to $4/2175$, so that the Reynolds number $Re = \mu^{-1} \int_{\Gamma_{in}} \vec{v} \cdot \vec{n} ds$ based on the flux at the inflow, is equal to 58.

We consider the (global) functional $J(U)$ associated with the kinetic energy over the whole domain Ω

$$E_{kin} = \frac{1}{2} \int_{\Omega} |\vec{v}|^2 d\Omega. \quad (69)$$

We employ ALGORITHM 5.1: in particular, for generating the successive grids, we adopt the metric \widetilde{M}_v only, for a target number of elements fixed to 3000. Figure 3 gathers the initial grid (top-left) together with the adapted meshes yielded by the first three iterations of the procedure. The final mesh (bottom-center) highlights the regions which most influence the computation of the kinetic energy: we recall that the orientation and the stretching of the elements depend

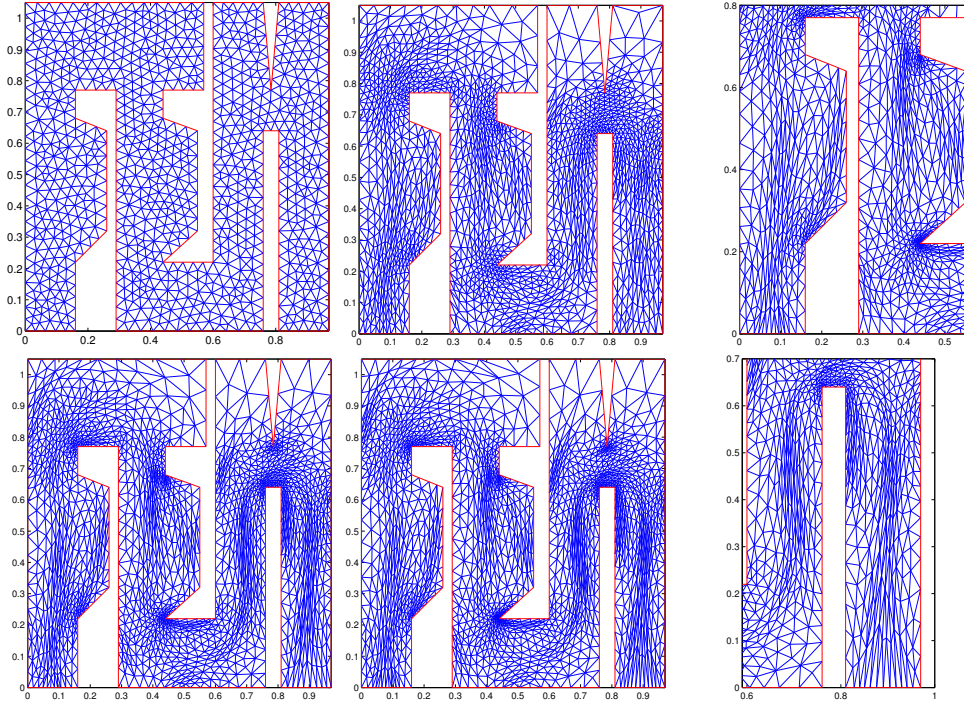


Figure 3: Brenner & Scott test case with $J(U) = E_{kin}$, $Re = 58$, and a target number of elements fixed to 3000. Sequence of adapted meshes: initial (top-left), first (top-center), second (bottom-left) and third adapted grid (bottom-center). Details of the third adapted mesh (top-right and bottom-right).

on the weighted Hessian, merging the primal and dual contributions of the errors on the velocities, and that the area of the triangles is inversely proportional to the size of the residuals (see, e.g., (54)). Note that there are zones, such as the ones on top of the domain, which contribute less, as the main bendy flow skips them. The two figures on the right of Figure 3 zoom in on some details of the last adapted mesh: in more detail, the lateral expansions characterizing the F and E letters (top-right) emphasize the presence of recirculation, while the two legs of the M (bottom-right) stress the bendy pattern of the main flow.

As a second run we decrease by a factor 5 the viscosity, so that the Reynolds number grows five times as large as in the previous case, i.e., $Re = 290$. The same velocity profiles are enforced at both the inflow and outflow sections. The initial mesh (top-left) plus the three resulting adapted meshes are collected in Figure 4 (left and center) as well as some details (right). On contrasting the two final (bottom-center) meshes in Figures 3-4 as well as their corresponding zoomed details, we observe that, in the case of the higher Reynolds number, the flow strengthens and straightens out, exhibiting a trend away from the lateral zones. Moreover, after the final turn, the higher velocity causes the flow to hit

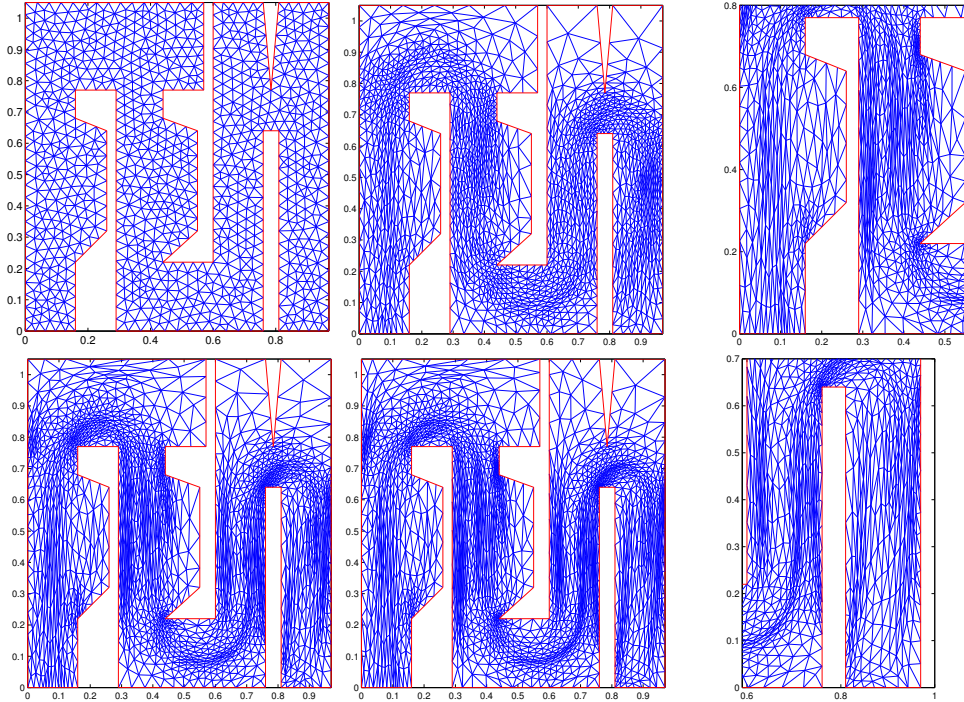


Figure 4: Brenner & Scott test case with $J(U) = E_{kin}$, $Re = 290$, and a target number of elements fixed to 3000. Sequence of adapted meshes: initial (top-left), first (top-center), second (bottom-left) and third adapted grid (bottom-center). Details of the third adapted mesh (top-right and bottom-right).

on the vertical border of the domain before coming back towards the center of the channel. The structure of the adapted mesh is also different: in the right M leg of Figure 3 the elements cluster around the center of the pipe, while in Figure 4 around the lateral boundaries.

6.2 The double ring test case

We consider a test case where the anisotropic features of the solution are emphasized. In particular we let the domain $\Omega = (0, 1)^2$, $\mu = 0.01$, and we choose the source term \vec{f} such that the exact solution (\vec{v}, p) , with $\vec{v} = [v_r, v_\theta]^T$, in polar coordinates pinned at $(0.5, 0.5)$, coincides with

$$v_r = 0, \quad v_\theta = \exp \left[- \left(\frac{r - r_1}{\delta} \right)^2 \right] + \exp \left[- \left(\frac{r - r_2}{\delta} \right)^2 \right], \quad p = 0,$$

with $r = \sqrt{(x_1 - 0.5)^2 + (x_2 - 0.5)^2}$, $r_1 = 0.15$, $r_2 = 0.3$ and $\delta = 0.01$. The flow field describes two thin concentric ring-like vortices, whose width is $\mathcal{O}(\delta)$ around $r = r_1$ and $r = r_2$, respectively. This flow may arise, for instance, due to

the effect of a particular wind pattern, or of a stirring force modeled by \vec{f} . The Reynolds number computed as $Re = \max_r v_\theta(r)r_2/\mu$ is equal to 30.

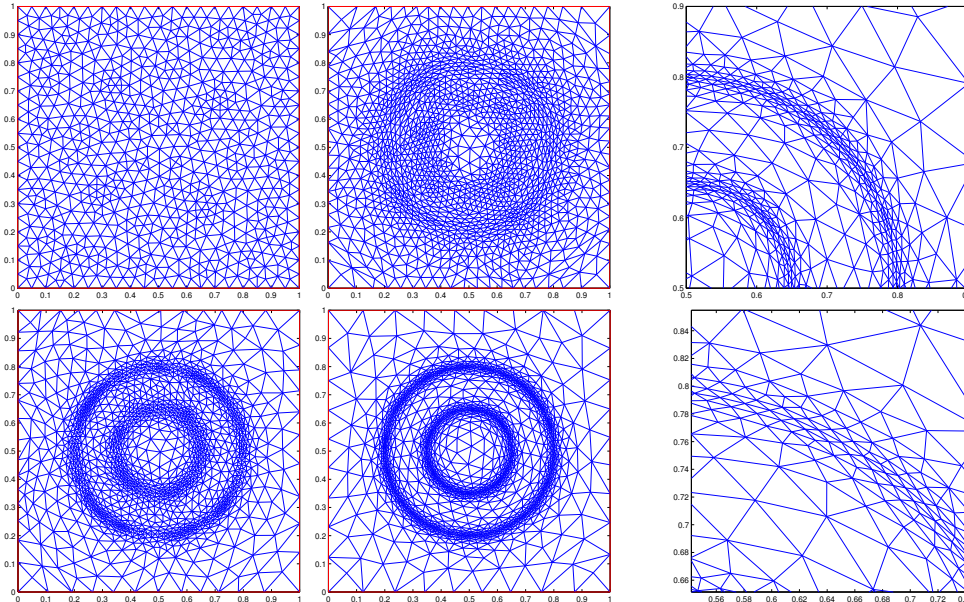


Figure 5: Double ring test case with $J(U) = E_{kin}$, $Re = 30$, and a target number of elements equal to 3000. Sequence of adapted meshes: initial (top-left), first (top-center), second (bottom-left) and sixth adapted grid (bottom-center). Particulars of the last adapted mesh (top-right and bottom-right).

We are interested in computing the total kinetic energy of the fluid so that the functional $J(\cdot)$ still coincides with (69). ALGORITHM 5.1 is adopted and only the metric \bar{M}_v is employed for driving the adaptive process, tuned on a desired number of elements equal to 3000. Figure 5 collects the initial mesh (top-left), along with the first (top-center), second (bottom-left) and sixth (bottom-center) adapted mesh. In the two zooms on the left, one can appreciate that the directional features of the velocity field are quickly captured by the adaptive procedure: a few iterations suffice to get a quite accurate approximation of the two vortices, and the mesh elements follow closely the tangential behavior of the flow pattern.

6.3 The flow past a cylinder test case

This test case represents a typical benchmark problem for the Navier-Stokes equations ([30]). It aims at computing both the lift and drag coefficients for a cross-section of a cylinder in a channel flow. This allows us to investigate the adaptive procedure in a situation where the functional $J(\cdot)$ has a local nature as

well as the dual problem is fed on nonhomogeneous Dirichlet conditions different from the ones pertaining to the primal problem.

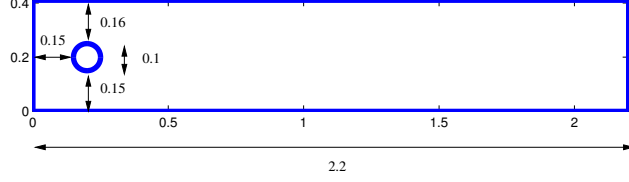


Figure 6: Domain Ω for the flow past a cylinder test case.

The computational domain Ω is a rectangular channel, with a width $H = 0.41$, drilled with a circular hole representing the cross-section of a cylinder and characterized by a slightly asymmetric configuration (see Figure 6). The boundary conditions are prescribed as follows: on the inflow section $\Gamma_{in} = \{x_1 = 0\} \cap \{0 < x_2 < H\}$, $\vec{v} = [v_{in}, 0]^T$, with $v_{in} = 4U_m x_2(H - x_2)/H^2$ the inlet parabolic profile, and $U_m = 0.3$ the peak velocity; on the outlet section $\Gamma_{out} = \{x_1 = 2.2\} \cap \{0 < x_2 < H\}$ the zero-traction condition $\boldsymbol{\sigma}\vec{n} = \vec{0}$ applies, while on the remaining rigid walls $\Gamma_{cyl} \cup \Gamma_{wall}$, the no-slip constraint $\vec{v} = \vec{0}$ holds, where $\Gamma_{cyl}, \Gamma_{wall}$ denote the cylinder and horizontal boundary, respectively. The viscosity is equal to $\mu = 0.001$, such that the Reynolds number $Re = \bar{v}D/\mu$ based on the mean velocity $\bar{v} = 0.2$ and on the cylinder diameter $D = 0.1$, amounts to 20. The body force \vec{f} vanishes everywhere. The chosen functionals

$$J_{drag} = c_0 \int_{\Gamma_{cyl}} \boldsymbol{\sigma}(\vec{v}, p)\vec{n} \cdot \vec{1}_{\parallel} ds \quad \text{and} \quad J_{lift} = c_0 \int_{\Gamma_{cyl}} \boldsymbol{\sigma}(\vec{v}, p)\vec{n} \cdot \vec{1}_{\perp} ds, \quad (70)$$

represent the so-called drag and lift coefficients, where $\vec{1}_{\parallel}, \vec{1}_{\perp}$ are the unit vectors parallel and orthogonal, respectively to the main flow direction (the horizontal one), with $c_0 = 2/D\bar{v}^2$. As observed in [18, 2], the employment of (70) does not yield accurate results, due to the need of computing numerically first-order derivatives along the cylinder. A more stable and accurate form is obtained by resorting to an interior rather than a boundary integral. In particular, if we define the two vector fields

$$\vec{w}_{drag} = \begin{cases} [1, 0]^T & \text{on } \Gamma_{cyl} \\ \vec{0} & \text{on } \partial\Omega \setminus \Gamma_{cyl} \end{cases} \quad \text{and} \quad \vec{w}_{lift} = \begin{cases} [0, 1]^T & \text{on } \Gamma_{cyl} \\ \vec{0} & \text{on } \partial\Omega \setminus \Gamma_{cyl}, \end{cases} \quad (71)$$

associated with the drag and the lift, respectively, it is possible to replace (70) by the equivalent form

$$J_{drag} = c_0 a(U)(Z_d) \quad \text{and} \quad J_{lift} = c_0 a(U)(Z_l), \quad (72)$$

where $a(U)(\cdot)$ is defined in (34), $Z_d = [\vec{w}_{drag}, 0]^T$, $Z_l = [\vec{w}_{lift}, 0]^T$. The vector fields \vec{w}_{drag} and \vec{w}_{lift} can thus be profitably thought of as dual velocity fields

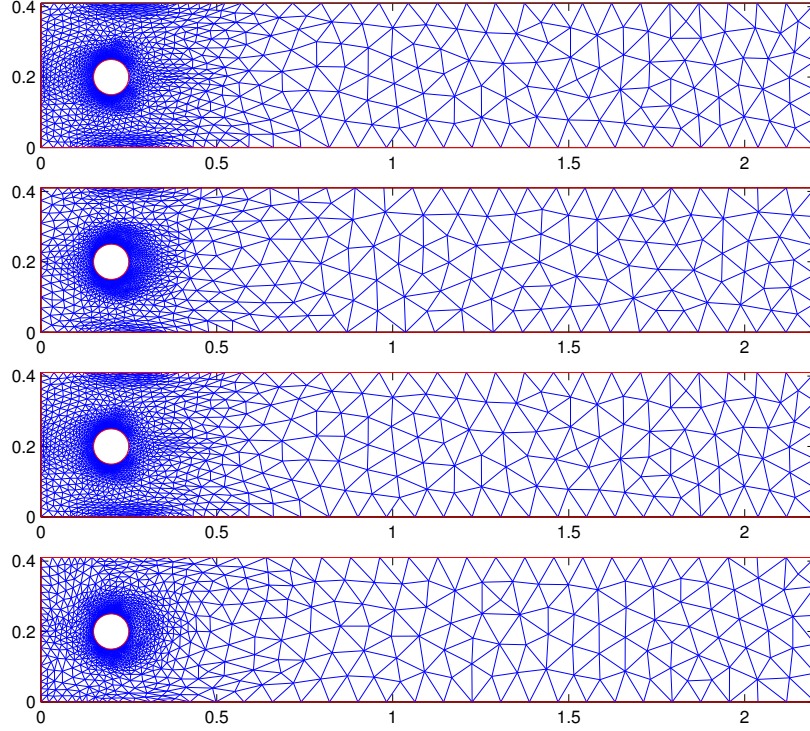


Figure 7: Flow past a cylinder test case for the drag (first and third row) and the lift (second and fourth row) coefficients, with $Re = 20$ and a target number of 3000 elements. Sequence of the third (final) adapted meshes: optimal metric driven by \widetilde{M}_v (first and second row) and by \widetilde{M}_p (third and fourth row).

satisfying the boundary conditions (71), or, likewise, as suitable extensions into Ω of the two unit vectors $\vec{1}_{\parallel}, \vec{1}_{\perp}$, respectively. The dual problem is consequently obtained after choosing the data $\mathbf{j}_w = \vec{0}$, $j_r = 0$ in (35), completed with the boundary conditions (71). The approximate counterpart of the expressions (72) is then obtained by replacing each variable with its corresponding numerical approximation, i.e., as

$$J_{drag,h} = c_0 a(U_h)(Z_{d,h}) \quad \text{and} \quad J_{lift,h} = c_0 a(U_h)(Z_{l,h}), \quad (73)$$

with $U_h = [\vec{v}_h, p_h]^T$ the primal pair, and $Z_{d,h}, Z_{l,h}$ the discrete dual solutions corresponding to Z_d and Z_l , respectively.

We apply ALGORITHM 5.1 by comparing its performance according to both the choices \widetilde{M}_v and \widetilde{M}_p in view of the optimal metric. The target number of elements is always set to 3000. We gather the results of the simulations in Figure 7: it shows the final (third) adapted mesh associated with the drag (first and third row) and with the lift (second and fourth row) corresponding to \widetilde{M}_v (first and second row) and to \widetilde{M}_p (third and fourth row).

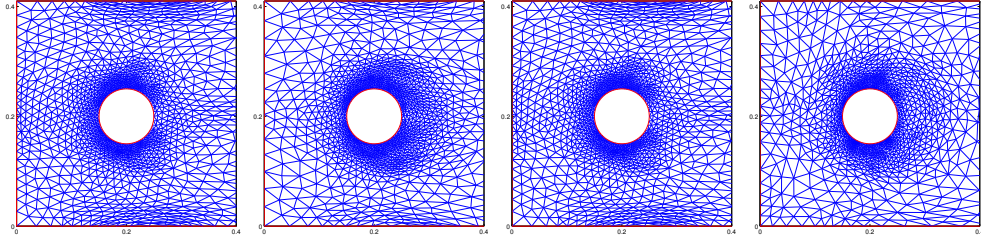


Figure 8: Flow past a cylinder test case for the drag (first and third column) and the lift (second and fourth column) coefficients, with $Re = 20$ and a target number of 3000 elements. Details of the third (final) adapted meshes: optimal metric driven by \widetilde{M}_v (first and second column) and by \widetilde{M}_p (third and fourth column).

Table 1: Computation of the drag and lift coefficients: drag (first column), error on the drag (second column); lift (third column), error on the lift (fourth column); optimal metric equal to \widetilde{M}_v (top) and to \widetilde{M}_p (bottom).

	$J_{d,h}$	$ J_d - J_{d,h} $	$J_{l,h}$	$ J_l - J_{l,h} $
\widetilde{M}_v	$5.5437 \cdot 10^{+0}$	$3.5835 \cdot 10^{-2}$	$1.0345 \cdot 10^{-2}$	$2.7399 \cdot 10^{-4}$
\widetilde{M}_p	$5.5463 \cdot 10^{+0}$	$3.3235 \cdot 10^{-2}$	$1.0253 \cdot 10^{-2}$	$3.6600 \cdot 10^{-4}$

A zoom around the cylinder of the four adapted meshes in Figure 7 is collected in Figure 8. We can observe that, as far as both coefficients are concerned, the employment of the pressure based metric \widetilde{M}_p allows for a less clustering of the mesh elements around the cylinder, while for a fixed metric, both Figures 7 and 8 highlight that the pattern of the mesh associated with the lift exhibits, on the one hand, some refinement in a wider area downwind the cylinder, but on the other hand, a more stressed coarseness upwind the cylinder.

The numerical values of the coefficients J_{drag} and J_{lift} obtained through (73) are shown in Table 1. The errors are obtained using the reference values, correct up to seven digits, $J_{drag} = 5.579535$ and $J_{lift} = 0.010619$ cited in [3]. Firstly we point out that, as the lift coefficient is two order of magnitude smaller than the drag coefficient, it is quite difficult to achieve a relative error smaller than 1% for both quantities ([2]). The observed relative errors are of the order of 0.6% and 3% for the drag and lift, respectively; we also emphasize that these results are obtained with as few elements as about 3000. Moreover, the numerical computation of the coefficients does not seem to depend much on the type of metric employed.

Appendix: Subgrid stabilization

Let us briefly discuss the subgrid stabilization of (9) under the hypothesis $V_0 = V = W = W_0$. The idea is to split the exact solution $u \in V$ as $u = u_h + u_B$, where $u_h \in V_h$ is the computable (finite dimensional) approximation and $u_B \in V_B$ is the subgrid correction (which is supposed to be unresolved by the current grid, infinite dimensional and “small”), and $V = V_h \oplus V_B$. Moreover, it turns out that $V_B = \prod_{K \in \mathcal{T}_h} H_0^1(K)$, that is, the subgrid-scale space comprises infinite dimensional “bubble” functions, one for each mesh element ([7]). Then it follows that

$$\langle \mathcal{A}(u_h + u_B), v_h + v_B \rangle = \langle f, v_h + v_B \rangle \quad \forall v_h \in V_h, \quad \forall v_B \in V_B,$$

v_h, v_B being the corresponding computable and unresolved test functions. Using the first order Taylor expansion $\mathcal{A}(u_h + u_B) \simeq \mathcal{A}(u_h) + \mathcal{A}'(u_h)u_B$, and taking into account the independence of v_h and v_B , we obtain the split problems

$$\begin{aligned} \langle \mathcal{A}(u_h) + \mathcal{A}'(u_h)u_B, v_h \rangle &= \langle f, v_h \rangle \quad \forall v_h \in V_h, \\ \langle \mathcal{A}(u_h) + \mathcal{A}'(u_h)u_B, v_B \rangle &= \langle f, v_B \rangle \quad \forall v_B \in V_B. \end{aligned} \tag{74}$$

The idea is to solve, in an approximate fashion, (74)₂ for u_B in terms of u_h and to plug the resulting expression back into (74)₁ in view of a single equation for u_h only. Thus we have

$$\langle \mathcal{A}'(u_h)u_B, v_B \rangle = \langle f - \mathcal{A}(u_h), v_B \rangle \quad \forall v_B \in V_B,$$

and, picking v_B independently on each triangle K , we obtain

$$\mathcal{A}'(u_h)u_B = f - \mathcal{A}(u_h) \quad \forall K \in \mathcal{T}_h.$$

It follows that

$$u_B = [\mathcal{A}'(u_h)]^{-1} (f - \mathcal{A}(u_h)) \simeq \tau_K (f - \mathcal{A}(u_h)) \quad \forall K \in \mathcal{T}_h, \tag{75}$$

with τ_K a suitable approximation to $[\mathcal{A}'(u_h)]^{-1}$, typically in algebraic form. Using the definition of the adjoint operator, the computable problem (74)₁ can be rewritten as

$$\langle \mathcal{A}(u_h), v_h \rangle + \langle u_B, \mathcal{A}'(u_h)^* v_h \rangle = \langle f, v_h \rangle \quad \forall v_h \in V_h,$$

namely, thanks to (75),

$$\langle \mathcal{A}(u_h), v_h \rangle + \langle f - \mathcal{A}(u_h), \mathcal{A}'(u_h)^* v_h \rangle_\tau = \langle f, v_h \rangle \quad \forall v_h \in V_h,$$

the definition (19) having also been employed.

As for the dual problem (16), we can proceed similarly, except that now the problem is linear. Firstly, as we are actually interested in the discrete dual

problem, we approximate u through u_h , then we introduce the decomposition $z = z_h + z_B$, with $z_h \in V_h$ and $z_B \in V_B$, from which we get the split problems

$$\begin{aligned}\langle \mathcal{A}'(u_h)^*(z_h + z_B), v_h \rangle &= \langle j, v_h \rangle \quad \forall v_h \in V_h, \\ \langle \mathcal{A}'(u_h)^*(z_h + z_B), v_B \rangle &= \langle j, v_B \rangle \quad \forall v_B \in V_B.\end{aligned}\tag{76}$$

The problem for the unresolved part is then

$$\langle \mathcal{A}'(u_h)^* z_B, v_B \rangle = \langle j - \mathcal{A}'(u_h)^* z_h, v_B \rangle \quad \forall v_B \in V_B,$$

whose elementwise solution is given by

$$z_B = [\mathcal{A}'(u_h)^*]^{-1}(j - \mathcal{A}'(u_h)^* z_h) \simeq \tau_K^*(j - \mathcal{A}'(u_h)^* z_h) \quad \forall K \in \mathcal{T}_h,$$

τ_K^* being a suitable approximation on K to $[\mathcal{A}'(u_h)^*]^{-1}$. The final form of the computable problem (76)₁ is thus

$$\langle \mathcal{A}'(u_h)^* z_h, v_h \rangle + \langle j - \mathcal{A}'(u_h)^* z_h, \mathcal{A}'(u_h) v_h \rangle_{\tau^*} = \langle j, v_h \rangle \quad \forall v_h \in V_h.$$

Summing up what we have obtained so far, we gather the primal and dual problems for the resolvable scales as

$$\begin{aligned}\langle \mathcal{A}(u_h), v_h \rangle + \langle f - \mathcal{A}(u_h), \mathcal{A}'(u_h)^* v_h \rangle_{\tau} &= \langle f, v_h \rangle \quad \forall v_h \in V_h \\ \langle \mathcal{A}'(u_h)^* z_h, v_h \rangle + \langle j - \mathcal{A}'(u_h)^* z_h, \mathcal{A}'(u_h) v_h \rangle_{\tau^*} &= \langle j, v_h \rangle \quad \forall v_h \in V_h\end{aligned}\tag{77}$$

with $\tau_K \simeq [\mathcal{A}'(u_h)]^{-1}$ and $\tau_K^* \simeq [\mathcal{A}'(u_h)^*]^{-1}$ on K .

Comparing (77) with (21), we deduce that, in the case of subgrid stabilization, it holds

$$\mathcal{S}_p(u_h) = -\mathcal{A}'(u_h)^* \quad \text{and} \quad \mathcal{S}_d(u_h) = -\mathcal{A}'(u_h),$$

the piecewise stability constants τ_K, τ_K^* being taken equal.

Acknowledgments. The authors thank Professor L.R. Scott for providing us with the details about the first test case.

References

- [1] T. APEL, *Anisotropic Finite Elements: Local Estimates and Applications*, Advances in Numerical Mathematics, Teubner, Stuttgart, 1999.
- [2] W. BANGERTH AND R. RANNACHER, *Adaptive Finite Element Methods for Differential Equations*, Lectures in Mathematics, ETH Zürich, Basel, Birkhäuser Verlag, 2003.
- [3] R. BECKER, *An optimal-control approach to a-posteriori error estimation for finite element discretizations of the Navier-Stokes equations*, East-West J. Numer. Math., 8(4) (2000), pp. 257–342.

- [4] R. BECKER, *Mesh adaption for stationary flow control*, J. Math. Fluid Mech., 3 (2001), pp. 317–341.
- [5] R. BECKER AND R. RANNACHER, *An optimal control approach to a posteriori error estimation in finite element methods*, Acta Numer., 10 (2001), pp. 1–102.
- [6] S.C. BRENNER AND L.R. SCOTT, *The Mathematical Theory of Finite Element Methods*, Springer-Verlag, New York, 1994.
- [7] F. BREZZI, L.P. FRANCA, T.J.R. HUGHES, AND A. RUSSO, $b = \int g$, Comput. Methods Appl. Mech. Engrg., 145 (1997), pp. 329–339.
- [8] M.J. CASTRO-DÍAZ, F. HECHT, B. MOHAMMADI, AND O. PIRONNEAU, *Anisotropic unstructured mesh adaption for flow simulations*, Internat. J. Numer. Methods Fluids, 25(4) (1997), pp. 475–491.
- [9] PH. CIARLET, *The Finite Element Method for Elliptic Problems*, North-Holland Publishing Company, Amsterdam, 1978.
- [10] PH. CLÉMENT, *Approximation by finite element functions using local regularization*, RAIRO Anal. Numér., 2 (1975), pp. 77–84.
- [11] D.L. DARMOFAL AND D.A. VENDITTI, *Grid adaption for functional outputs: application to two-dimensional inviscid fluids*, J. Comput. Phys., 176 (1) (2002), pp. 40–69.
- [12] J. DOMPIERRE, M.-G. VALLET, Y. BOURGAULT, M. FORTIN, AND W.G. HABASHI, *Anisotropic mesh adaptation: towards user-independent, mesh-independent and solver-independent CFD. Part III. Unstructured meshes*, Internat. J. Numer. Methods Fluids, 39 (2002), pp. 675–702.
- [13] M.B. GILES AND N.A. PIERCE, *Adjoint equation in CFD: duality, boundary conditions and solution behaviour*, AIAA Paper, 97-1850 (1997).
- [14] L. FORMAGGIA AND S. PEROTTO, *New anisotropic a priori error estimates*, Numer. Math., 89 (2001), pp. 641–667.
- [15] L. FORMAGGIA AND S. PEROTTO, *Anisotropic error estimates for elliptic problems*, Numer. Math., 94 (2003), pp. 67–92.
- [16] L.P. FRANCA AND S.L. FREY, *Stabilized finite element methods. II. The incompressible Navier-Stokes equations*, Comput. Methods Appl. Mech. Engrg., 99 (1992), pp. 209–233.
- [17] P.-L. GEORGE AND H. BOROUCAKI, *Delaunay Triangulation and Meshing. Application to Finite Elements*, Editions Hermés, 1998.

- [18] M.B. GILES AND E. SÜLI, *Adjoint methods for PDEs: a posteriori error analysis and postprocessing by duality*, Acta Numer., 11 (2002), pp. 145–236.
- [19] V. GIRAULT AND P.A. RAVIART, *Finite Element Methods for Navier Stokes Equations. Theory and Algorithms*, Springer Series in Computational Mathematics 5, Springer-Verlag, Berlin, Heidelberg, 1986.
- [20] G.H. GOLUB AND C.F. VAN LOAN, *Matrix Computations*, Second ed., The Johns Hopkins University Press, Baltimore, MD, 1996.
- [21] F. HECHT, *BAMG: Bidimensional Anisotropic Mesh Generator*, INRIA Report (1998), <http://www.inria.fr/>.
- [22] L.D. LANDAU AND E.M. LIFSHITZ *Fluid Mechanics*, Volume 6, Pergamon Press, London, 1959.
- [23] J.L. LIONS AND E. MAGENES, *Non-Homogeneous Boundary Value Problems and Applications*, Volume I, Springer-Verlag, Berlin, 1972.
- [24] J. LUBLINER *Plasticity Theory*, Macmillan, New York, 1990.
- [25] G.I. MARCHUK, *Adjoint Equations and Analysis of Complex Systems*, Kluwer Academic Publishers, Dordrecht, 1995.
- [26] S. MICHELETTI AND S. PEROTTO, *Reliability and efficiency of an anisotropic Zienkiewicz-Zhu error estimator*, Comput. Methods Appl. Mech. Engrg., 195(9–12) (2006), pp. 799–835.
- [27] S. MICHELETTI, S. PEROTTO, AND M. PICASSO, *Stabilized finite elements on anisotropic meshes: a priori error estimates for the advection-diffusion and Stokes problems*, SIAM J. Numer. Anal., 41 (2003), pp. 1131–1162.
- [28] J.T. ODEN AND S. PRUDHOMME, *Goal-oriented estimation and adaptivity for the finite element method*, Comput. Math. Appl., 41 (2001), pp. 735–756.
- [29] R. RODRIGUEZ, *Some remark on the Zienkiewicz–Zhu estimator*, Numer. Meth. Partial Diff. Eq.s, 10 (1994), pp. 625–635.
- [30] M. SCHÄFER AND S. TUREK, *Benchmark computations of laminar flow around a cylinder*, in NNFM 52 “Flow Simulation on High-Performance Computers II”, Vieweg, Braunschweig, 1996.
- [31] S. SELBERHERR, *Analysis and Simulation of Semiconductor Devices*, Springer Verlag, Wien, 1984.
- [32] K.G. SIEBERT, *An a posteriori error estimator for anisotropic refinement*, Numer. Math., 73 (1996), pp. 373–398.
- [33] R. TEMAM, *Navier-Stokes Equations. Theory and Numerical Analysis*, North-Holland, Amsterdam, 1984.

- [34] R. VERFÜRTH, *A Review of A Posteriori Error Estimation and Adaptive Mesh-Refinement Techniques*, Wiley-Teubner, New York, 1996.
- [35] O.C. ZIENKIEWICZ AND J.Z. ZHU, *The superconvergent patch recovery and a posteriori error estimates. Part 1: the recovery technique*, Int. J. Numer. Methods Engrg., 33 (1992), pp. 1331–1364.
- [36] O.C. ZIENKIEWICZ AND J.Z. ZHU, *The superconvergent patch recovery and a posteriori error estimates. Part 2: error estimates and adaptivity*, Int. J. Numer. Methods Engrg., 33 (1992), pp. 1365–1382.

MOX Technical Reports, last issues

Dipartimento di Matematica “F. Brioschi”,
Politecnico di Milano, Via Bonardi 9 - 20133 Milano (Italy)

- 18/2007 S. MICHELETTI, S. PEROTTO :
Output functional control for nonlinear equations driven by anisotropic mesh adaption. The Navier-Stokes equations
- 17/2007 A. DECOENE, L. BONAVENTURA, E. MIGLIO, F. SALERI:
Asymptotic Derivation of the Section-Averaged Shallow Water Equations for River Hydraulics
- 16/2007 A. QUARTERONI:
Modellistica Matematica e Calcolo Scientifico
- 15/2007 C. VERGARA, P. ZUNINO:
Multiscale modeling and simulation of drug release from cardiovascular stents
- 14/2007 L. DEDÉ:
Reduced Basis Method for Parametrized Advection-Reaction Problems
- 13/2007 P. ZUNINO:
Discontinuous Galerkin methods based on weighted interior penalties for second order PDEs with non-smooth coefficients
- 12/2007 A. DEPONTI, L. BONAVENTURA, G. ROSATTI, G. GAREGNANI:
An Accurate and Efficient Semi-Implicit Method for Section Averaged Free Surface Flow Modelling
- 11/2007 S. BADIA, F. NOBILE, C. VERGARA:
Fluid-structure partitioned procedures based on Robin transmission conditions
- 10/2007 N. PAROLINI, A. QUARTERONI:
Modelling and Numerical Simulation for Yacht Engineering
- 09/2007 C. MAY, N. FLOURNOY:
Asymptotics in response-adaptive designs generated by a two-colors, randomly reinforced urn